Numerical solution of the nonequilibrium square-gradient model and verification of local equilibrium for the Gibbs surface in a two-phase binary mixture

K. S. Glavatskiy[1] and D. Bedeaux[1,2]
[1]*Department of Chemistry, Norwegian University of Science and Technology, Trondheim, Norway*
[2]*Engineering Thermodynamics, Delft University of Technology, Leeghwaterstreet 44, 2628 CA, The Netherlands*
(Received 23 December 2008; published 31 March 2009)

In this paper we apply the general analysis described in our first paper to a binary mixture of cyclohexane and *n*-hexane. We use the square gradient model for the continuous description of a nonequilibrium surface and obtain numerical profiles of various thermodynamic quantities in various stationary state conditions. Details of the numerical procedure are given and discussed. In the second part of this paper we focus on the verification of local equilibrium of the surface as described with excess densities. We give a definition of the temperature and chemical potentials of the surface and verify that these quantities are independent of the choice of the dividing surface. We verify numerically that the surface in a stationary state of the mixture can be described in terms of Gibbs excess densities, which are found to be in good approximation equal to their equilibrium values at the stationary state temperature and chemical potentials of the surface.

DOI: 10.1103/PhysRevE.79.031608 PACS number(s): 68.03.Fg, 05.70.Np, 65.40.gp, 64.70.F−

I. INTRODUCTION

In a previous article [1] we have established the square gradient description of the interface between two phases in nonequilibrium mixtures. We considered temperature, density, and mass fraction gradients; heat and diffusion fluxes as well as evaporation or condensation fluxes through the interface. Some profiles were given in [1], without going into details of the numerical procedures used to obtain them. In this paper we will do this.

In the general description of the interface one uses contributions to the Helmholtz free energy density proportional to the square of the density and mass fraction gradients. These contributions imply that it is not possible to use *continuous local equilibrium thermodynamics* in the interfacial region, i.e., to calculate the local values of the various thermodynamic parameters in terms of the local density, mass fractions, and temperature only. Rowlinson and Widom (see [2], p. 43) use the name *point thermodynamics* for this, to distinguish it from other *quasi*-or *local thermodynamic* treatments. Given the nonautonomous nature of the square gradient model, it is sensible to question whether a description in terms of excess variables along the lines given by Gibbs [3] can be autonomous. Gibbs' treatment, though only given for equilibrium systems, suggests such an assumption. This would imply that the surface is a separate thermodynamic phase. Bakker [4] and Guggenheim ([5], p. 45) made this assumption, the validity of which was subsequently disputed by Defay and Prigogine [6]. We refer to Rowlinson and Widom ([2], p. 33) for a discussion of this point. In the theory of nonequilibrium thermodynamics of surfaces [7–10] Gibbs' description in terms of excess variables has been used. It is then assumed that Gibbs' description of the surface in terms of excess variables is autonomous, or in other words that one can use this property, which we will call *local equilibrium of the surface*, to describe the surface. In earlier work [11] coauthored by one of us, this property was verified for a one-component square-gradient system. It is the main objective of this paper to verify this property for binary mixtures. For details about the extension of the square-gradient model to nonequilibrium mixtures we refer to [1]. For figures of typical density, mass fraction, and temperature profiles, and a discussion thereof, we also refer to the first paper. In this paper we focus on the properties of the excess variables.

The validity of local equilibrium for a surface in a nonequilibrium mixture is a great simplification. Without this simplification the surface excess densities depend also on the values of the temperature and chemical potentials of the adjacent phases. This complicates the description to a level that is difficult to manage. Also the possibility to introduce and define a temperature and chemical potentials for the surface, which are independent of the location of the dividing surface chosen, is an important simplification. For the one-component system local equilibrium has been verified on the basis of both molecular dynamics simulations [12–14] and the nonequilibrium square-gradient model [11]. For binary mixtures a limited number of molecular dynamics simulations of evaporation and condensation have been done [15–18]. None are available which verify the property of local equilibrium, however. Establishing this property using the square-gradient model is therefore the only available option. For a proper understanding of an important industrial process such as distillation the validity of local equilibrium for the interface would be a great help. In this paper we succeed to prove this for a binary mixture. Given the validity for one- and two-component systems we feel confident to formulate the hypothesis that local equilibrium is valid for surfaces in nonequilibrium multicomponent mixtures.

We consider a flat interface between a binary liquid and its vapor with the normal $\mathbf{n}=(1,0,0)$ pointing from the vapor to the liquid. We choose all fluxes and gradients to be in the x direction. Due to this, all variables depend only on the x coordinate. To simplify the analysis we assume the fluid to be nonviscous, so that the viscous pressure tensor $\pi_{\alpha\beta}=0$. Neither the parallel nor the normal hydrostatic pressure are assumed to be constant.

In Sec. II we give all the equations which are required for the determination of the various profiles in stationary states

of the system. The numerical analysis of stationary states is a natural first step, as the numerical analysis of nonstationary states is much more involved. In the following section we shall give the various thermodynamic densities which follow from the van der Waals equation of state [1] and the gradient terms to be added in the interfacial region. We choose the system such that the gas is on the left-hand side and the liquid is on the right-hand side. The x axis is directed from left to right and the gravitational acceleration $\mathbf{g}$ is directed towards the liquid. The numerical solution is calculated between two points where boundary conditions are given. The region between these two points we refer to as the box. In Sec. III we describe the numerical procedure which has been used to solve these equations. We give the results in Sec. IV. We then proceed to the second part of the article, the verification of local equilibrium of the surface. In Sec. V we introduce excesses and surface variables and discuss in general the meaning of local equilibrium of the surface. In Sec. VI we give the results of the verification procedure. Finally, in Sec. VII we give concluding remarks.

II. COMPLETE SET OF EQUATIONS

We give the complete set of equations required to calculate the various profiles in the nonequilibrium mixture. This set is given by the hydrodynamic balance (conservation) equations, the thermodynamic equations of state, and the phenomenological force-flux relations. These equations were given (derived) and discussed in [1], to which we refer. In this paper we will only list them for the stationary case.

A. Conservation equations

In a stationary state the conservation equations take the following form: The law of mass conservation for the components give

$$\frac{d}{dx}(\rho \mathrm{v}) = 0,$$

$$\frac{d}{dx}(J_1 + \rho_1 \mathrm{v}) = \frac{d}{dx}(J_1 + \rho\xi \mathrm{v}) = 0, \tag{2.1}$$

where $\rho=\rho_1+\rho_2$ and $\mathrm{v}=(\rho_1\mathrm{v}_1+\rho_2\mathrm{v}_2)/\rho$ are the mass density and the barycentric (center of mass) velocity. Furthermore $\xi=\rho_1/\rho$ is the mass fraction of the first component and $J_1=\rho_1(\mathrm{v}_1-\mathrm{v})=\rho\xi(\mathrm{v}_1-\mathrm{v})$ is the diffusion flux of the first component relative to the barycentric frame of reference. The diffusion flux of the second component is $J_2=\rho_2(\mathrm{v}_2-\mathrm{v})=-J_1$. Momentum conservation is given by

$$\frac{d}{dx}(\rho \mathrm{v}^2 + p + \gamma_{xx}) = \rho g, \tag{2.2}$$

where $\gamma_{\alpha\beta}$ is called the thermodynamic tension tensor, which will be defined below. Furthermore p and $p+\gamma_{xx}$ are the pressures parallel and perpendicular to the interface, for the planar interface under consideration. For curved surfaces see our first paper [1]. Energy conservation is given by

$$\frac{d}{dx}J_e = 0, \tag{2.3}$$

where $J_e \equiv J_q + \rho e \mathrm{v} + pv$ is the total energy flux, J_q is the heat flux, $e=u+\mathrm{v}^2/2-gx$ is the total specific energy, and u is the specific internal energy.

B. Thermodynamic equations

The square gradient model, discussed in the first paper [1], gives the following expressions for the specific Helmholtz energy f, the specific internal energy u, the parallel pressure p, the *chemical potential difference*[1] $\psi \equiv \mu_1 - \mu_2$, the chemical potential of the second component $\mu \equiv \mu_2$, and the xx element of the tension tensor γ_{xx}:

$$f(x) = f_0(T,\rho,\xi) + \mathcal{K}(\rho,\xi,\rho',\xi'),$$

$$u(x) = f_0(T,\rho,\xi) - T\frac{\partial}{\partial T}f_0(T,\rho,\xi) + \mathcal{K}(\rho,\xi,\rho',\xi'),$$

$$p(x) = \rho^2\frac{\partial}{\partial\rho}[f_0(T,\rho,\xi) + \mathcal{K}(\rho,\xi,\rho',\xi')] - \rho\frac{d}{dx}\left(\rho\frac{\partial}{\partial\rho'}\mathcal{K}(\rho,\xi,\rho',\xi')\right),$$

$$\psi(x) = \frac{\partial}{\partial\xi}[f_0(T,\rho,\xi) + \mathcal{K}(\rho,\xi,\rho',\xi')] - \frac{1}{\rho}\frac{d}{dx}\left(\rho\frac{\partial}{\partial\xi'}\mathcal{K}(\rho,\xi,\rho',\xi')\right),$$

$$\mu(x) = \frac{\partial}{\partial\rho}\{\rho[f_0(T,\rho,\xi) + \mathcal{K}(\rho,\xi,\rho',\xi')]\} - \psi(x)\xi - \rho\frac{d}{dx}\left(\rho\frac{\partial}{\partial\rho'}\mathcal{K}(\rho,\xi,\rho',\xi')\right),$$

$$s(x) = -\frac{\partial}{\partial T}f_0(T,\rho,\xi),$$

$$\gamma_{xx}(x) = 2\rho\mathcal{K}(\rho,\xi,\rho',\xi'). \tag{2.4}$$

Here $f_0(T,\rho,\xi)=f_0^{\nu}(T,c,\zeta)$ is the specific Helmholtz energy of the homogeneous phase, which can for instance be derived from the equation of state. Furthermore $\mathcal{K}(\rho,\xi,\rho',\xi')$ is the gradient contribution, where the primes indicate a derivative with respect to x. Since the equation of state is usually given in molar quantities, it is convenient to use them here as well. Thus, $c=\rho/M$ is the molar concentration, $\zeta=\xi M/M_1$ is the molar fraction of the first component, where $M=M_1M_2/[M_1+\xi(M_2-M_1)]=M_2+\zeta(M_1-M_2)$ is the molar mass of the mixture, and M_1 and M_2 are molar masses of each component.

[1] We use this name lacking a better one

C. The Helmholtz energy of a homogeneous system

This energy is given by the following equation:

$$f_0^{\nu}(T,c,\zeta) = -RT\ln\left(\frac{e}{cN_A}\frac{w(T,\zeta)}{\Lambda^3(T,\zeta)}[1-B(\zeta)c]\right) - A(T,\zeta)c, \tag{2.5}$$

where the de Broglie wavelength Λ and the characteristic sum over internal degrees of freedom w are, respectively,

$$\Lambda(T,\zeta) = \hbar N_A\left(\frac{2\pi}{MRT}\right)^{1/2},$$

$$w(T,\zeta) = \left[\frac{w_1}{\zeta}\left(\frac{M_1}{M}\right)^{3/2}\right]^{\zeta}\left[\frac{w_2}{1-\zeta}\left(\frac{M_2}{M}\right)^{3/2}\right]^{1-\zeta}. \tag{2.6}$$

Expressions for the characteristic sums over internal degrees of freedom for each component, w_1 and w_2, are given in [1]. In this paper they are assumed to be independent of the temperature and the molar fractions, i.e., just constant numbers. Equation (2.5) together with Eq. (2.6) follow from the van der Waals equation of state.

The mixing rules for A and B are

$$A(T,\zeta) = a_{11}\zeta^2 + 2a_{12}\zeta(1-\zeta) + a_{22}(1-\zeta)^2,$$

$$B(\zeta) = b_1\zeta + b_2(1-\zeta), \tag{2.7}$$

with $a_{ij}=\sqrt{a_i a_j}$, where a_i as well as b_i is a coefficient of a pure component i. We will assume in this paper that all a_{ij} and b_i are independent of temperature.

D. The gradient contribution

This contribution is given by the following general expression for a binary mixture

$$\mathcal{K}(\rho,\xi,\rho',\xi') \equiv \frac{1}{2\rho}[\kappa_{\rho\rho}(\rho,\xi)\rho'^2 + 2\kappa_{\rho\xi}(\rho,\xi)\rho'\xi' + \kappa_{\xi\xi}(\rho,\xi)\xi'^2]. \tag{2.8}$$

The coefficients $\kappa_{\rho\rho}$, $\kappa_{\rho\xi}$, and $\kappa_{\xi\xi}$ can be expressed in the gradient coefficients $\kappa_{\rho_1\rho_1}$ and $\kappa_{\rho_2\rho_2}$ for components 1 and 2 in the following way (see [1] for details):

$$\kappa_{\rho\rho}(\rho,\xi) = (\kappa_{\rho_1\rho_1} - 2\kappa_{\rho_1\rho_2} + \kappa_{\rho_2\rho_2})\xi^2 + 2(\kappa_{\rho_1\rho_2} - \kappa_{\rho_2\rho_2})\xi + \kappa_{\rho_2\rho_2},$$

$$\kappa_{\rho\xi}(\rho,\xi) = (\kappa_{\rho_1\rho_1} - 2\kappa_{\rho_1\rho_2} + \kappa_{\rho_2\rho_2})\rho\xi + (\kappa_{\rho_1\rho_2} - \kappa_{\rho_2\rho_2})\rho,$$

$$\kappa_{\xi\xi}(\rho,\xi) = (\kappa_{\rho_1\rho_1} - 2\kappa_{\rho_1\rho_2} + \kappa_{\rho_2\rho_2})\rho^2, \tag{2.9}$$

where for the cross coefficient we use the mixing rule $\kappa_{\rho_1\rho_2} = \sqrt{\kappa_{\rho_1\rho_1}\kappa_{\rho_2\rho_2}}$ similar to the one for coefficients a_{ij}. In this paper we will assume $\kappa_{\rho_i\rho_j}$ to be independent of the densities.

With the above mixing rules the gradient contribution can be written in the form

$$\mathcal{K}(\rho,\xi,\rho',\xi') \equiv \frac{\kappa q'^2}{2\rho}, \tag{2.10}$$

where $\kappa \equiv \kappa_{\rho_2\rho_2}$ and $q \equiv \rho(1+\varepsilon_\kappa^m\xi)$, where $\varepsilon_\kappa^m \equiv \varepsilon_\kappa \equiv (\sqrt{\kappa_{\rho_1\rho_1}} - \sqrt{\kappa_{\rho_2\rho_2}})/\sqrt{\kappa_{\rho_2\rho_2}}$. Some of the quantities from Eq. (2.4) can be rewritten as

$$p(x) = p_0 - \kappa\left(\frac{1}{2}q'^2 + qq''\right),$$

$$\mu(x) = \mu_0 - \kappa q'',$$

$$\psi(x) = \psi_0 - \varepsilon_\kappa\kappa q'', \tag{2.11}$$

where p_0, μ_0, and ψ_0 are values of the corresponding quantities in the homogeneous phase, which are found from Eq. (2.4) by setting $\mathcal{K}=0$. For a one-component fluid q equals the density. For the two-component mixture q plays a similar role as the density for the one-component fluid. We shall therefore refer to q as the order parameter.

For the surface tension of the flat interface one may show, using Eq. (2.10) and Eq. (2.4), that in equilibrium

$$\gamma_{\rm eq} = \int dx\,\gamma_{xx,\rm eq}(x) = \int dx 2\rho\mathcal{K}_{\rm eq} = \kappa\int dx q'^2_{\rm eq}. \tag{2.12}$$

It follows that $\kappa_{\rho_i\rho_i}$ is proportional to the surface tension of the pure component γ_i. It follows therefore that as an estimate for ε_κ one may use the relation

$$\varepsilon_\kappa \simeq \sqrt{\frac{\gamma_1}{\gamma_2}} - 1. \tag{2.13}$$

In an organic mixture such as cyclohexane and n-hexane, a mixture we will study in more detail in this paper, the components are very similar and as a consequence $|\varepsilon_\kappa|$ is small, as one can see from Eq. (2.13). The order parameter is then in good approximation equal to the density. When the components are very different $|\varepsilon_\kappa|$ may be large and q may become in good approximation equal to the density of one of the components.

E. Phenomenological equations

In the first paper [1] we derived the general expression for the entropy production of a mixture in the interfacial region. For a binary mixture which has only gradients and fluxes in the x direction it takes, neglecting the viscous contribution, the following form:

$$\sigma = J_q\frac{d}{dx}\frac{1}{T} - J_1\frac{d}{dx}\frac{\psi}{T}, \tag{2.14}$$

where we used $J_2=-J_1$. The resulting linear force-flux relations are

$$\frac{d}{dx}\frac{1}{T} = R_{qq}J_q - R_{q1}J_1,$$

$$\frac{d}{dx}\frac{\psi}{T} = R_{1q}J_q - R_{11}J_1. \tag{2.15}$$

The resistivity coefficients R_{qq}, R_{11}, and $R_{q1}=R_{1q}$ will in general depend on the densities, their gradients, as well as on the temperature, so they vary through the interface. Expressions for the resistivity profiles in the interfacial region are not available. We model them, using the bulk values as the limiting value away from the surface and the order parameter profile as a modulatory curve,

$$\begin{aligned} R_{qq}(x) &= R^g_{qq} + (R^\ell_{qq} - R^g_{qq})q_0(x) + \alpha_{qq}(R^\ell_{qq} + R^g_{qq})q_1(x), \\ R_{q1}(x) &= R^g_{q1} + (R^\ell_{q1} - R^g_{q1})q_0(x) + \alpha_{q1}(R^\ell_{q1} + R^g_{q1})q_1(x), \\ R_{11}(x) &= R^g_{11} + (R^\ell_{11} - R^g_{11})q_0(x) + \alpha_{11}(R^\ell_{11} + R^g_{11})q_1(x), \end{aligned} \tag{2.16}$$

where

$$q_0(x) = \frac{q(x) - q^g_{\mathrm{eq}}}{q^\ell_{\mathrm{eq}} - q^g_{\mathrm{eq}}}, \quad q_1(x) = \frac{|q'(x)|^2}{|q'_{\mathrm{eq}}(x)|^2_{\max}} \tag{2.17}$$

are modulatory curves for resistivity profiles. Here q^g_{eq} and q^ℓ_{eq} are the equilibrium coexistence values of the order parameter of the gas and liquid, respectively. Furthermore $|q'_{\mathrm{eq}}(x)|^2_{\max}$ is the maximum value of the squared equilibrium order parameter gradient. For each resistivity profile R^g and R^ℓ are the equilibrium coexistence resistivities of the gas and liquid phase, respectively. Coefficients α_{qq}, α_{q1}, α_{11} control the size of the gradient term, which gives peaks in the resistivity profiles in the interfacial region. Such a peak is observed in molecular dynamic simulations of one-component fluids [19].

Limiting coefficients R^b (where b is either g or ℓ) are related to measurable transport coefficients in the bulk phases: thermal conductivity λ^b, diffusion coefficient D^b, and Soret coefficient s^b_T. In the description of transport in the *homogeneous* phases it is convenient to use measurable heat fluxes

$$J'^b_q = J^b_q - J^b_1(h^b_1 - h^b_2), \tag{2.18}$$

where h^b_i is a specific enthalpy of component i in phase b. Furthermore we used $J^b_2=-J^b_1$. In the homogeneous phases the entropy production then takes the following form:

$$\sigma = J'_q\frac{d}{dx}\frac{1}{T} - J_1\frac{1}{T}\frac{d\psi_T}{dx}, \tag{2.19}$$

where we have suppressed the superscript b for now. The subscript T of ψ indicates that the gradient is calculated keeping the temperature constant. Using the Gibbs-Duhem relation in a homogeneous phase at a constant pressure one can show

$$\frac{d\psi_T}{dx} = \frac{\partial\mu_1}{\partial\xi}\frac{1}{(1-\xi)}\frac{d\xi}{dx}. \tag{2.20}$$

After introducing measurable transport coefficients, the force-flux relations derived from Eq. (2.19) can be written in a form used in [20],

$$\begin{aligned} J'_q &= -\lambda\frac{dT}{dx} - \rho\xi\frac{\partial\mu_1}{\partial\xi}TDs_T\frac{d\xi}{dx}, \\ J_1 &= -\rho\xi(1-\xi)Ds_T\frac{dT}{dx} - \rho D\frac{d\xi}{dx}. \end{aligned} \tag{2.21}$$

Comparing Eq. (2.15) and Eq. (2.21) in the homogeneous region we find the values R of corresponding resistivity coefficients,

$$\begin{aligned} R_{qq} &= \frac{1}{LT^2}\frac{D\rho}{\psi_\xi}, \\ R_{q1} = R_{1q} &= \frac{1}{LT^2}\left(\frac{D\rho}{\psi_\xi}(h_1 - h_2) + Ds_T\rho\xi(1-\xi)T\right), \\ R_{11} &= \frac{1}{LT^2}\left(\frac{D\rho}{\psi_\xi}(h_1 - h_2)^2 + Ds_T\rho\xi(1-\xi)T(h_1 - h_2) + \lambda T\right), \end{aligned} \tag{2.22}$$

where $\psi_\xi=(\partial\psi/\partial\xi)$, $L=(\lambda D\rho/\psi_\xi)-[Ds_T\rho\xi(1-\xi)]^2T$. All the quantities in Eq. (2.22) are taken in the specified, either gas or liquid, phase.

III. SOLUTION PROCEDURE

The numerical procedure is similar to the one described in [21], however, it has some differences. We will describe the special features below. We use the MATLAB procedure bvp4c [22] to solve the stationary boundary value problem. This requires a reasonable initial guess as well as boundary conditions. We use the equilibrium profile as the initial guess. We use a box of width 80 nm with the grid containing 81 equidistantly spread points.

A. Equilibrium profile

It is easier to describe equilibrium properties of the mixture using molar quantities. In this section we will do this. The superscript ν indicates a molar quantity. The total molar concentration and molar fraction of the first component, denoted by c and ζ, respectively, were defined at the end of Sec. II B.

Equilibrium coexistence is determined by the following system of equations:

$$\begin{aligned} \mu^\nu_{\mathrm{eq}} &= \mu^\nu_0(T_{\mathrm{eq}}, c^g_{\mathrm{eq}}, \zeta^g_{\mathrm{eq}}) = \mu^\nu_0(T_{\mathrm{eq}}, c^\ell_{\mathrm{eq}}, \zeta^\ell_{\mathrm{eq}}), \\ \psi^\nu_{\mathrm{eq}} &= \psi^\nu_0(T_{\mathrm{eq}}, c^g_{\mathrm{eq}}, \zeta^g_{\mathrm{eq}}) = \psi^\nu_0(T_{\mathrm{eq}}, c^\ell_{\mathrm{eq}}, \zeta^\ell_{\mathrm{eq}}), \\ p_{\mathrm{eq}} &= p_0(T_{\mathrm{eq}}, c^g_{\mathrm{eq}}, \zeta^g_{\mathrm{eq}}) = p_0(T_{\mathrm{eq}}, c^\ell_{\mathrm{eq}}, \zeta^\ell_{\mathrm{eq}}), \end{aligned} \tag{3.1}$$

where $\psi^\nu_0=(\partial f^\nu_0/\partial\zeta)$, $\mu^\nu_0=f^\nu_0+c(\partial f^\nu_0/\partial c)-\psi^\nu_0\zeta$, and $p_0=c^2(\partial f^\nu_0/\partial c)$ are chemical potentials and pressure of the homogeneous phases. c^g_{eq}, ζ^g_{eq} and c^ℓ_{eq}, ζ^ℓ_{eq} are coexistence density and mass fractions of gas and liquid, respectively.

Having six equations, Eq. (3.1), and eight unknowns, c^g_{eq}, ζ^g_{eq}, c^ℓ_{eq}, ζ^ℓ_{eq}, ψ^ν_{eq}, μ^ν_{eq}, p_{eq}, T_{eq}, two of the unknowns need to

be specified for the two component mixture. The temperature and the pressure are experimentally a convenient choice. We have found, however, that it is more convenient to control $T_{\rm eq}$ and $\psi^{\nu}_{\rm eq}$ in the calculations, because $\psi^{\nu}_{\rm eq}$ changes monotonically with $\zeta^{g}_{\rm eq}$ or $\zeta^{\ell}_{\rm eq}$, and it is therefore a good measure for the composition. Since $\psi^{\nu}=\mu^{\nu}_1-\mu^{\nu}_2$, the value of ψ^{ν} gives the difference of the chemical potentials of two components.

To obtain the equilibrium profiles $c_{\rm eq}(x)$ and $\zeta_{\rm eq}(x)$ one needs to solve a system of two differential equations

$$\mu^{\nu}_{\rm eq} = \mu^{\nu}_0(c,\zeta) - \kappa^{\nu}(q^{\nu})'',$$

$$\psi^{\nu}_{\rm eq} = \psi^{\nu}_0(c,\zeta) - \varepsilon^{\nu}_{\kappa}\kappa^{\nu}(q^{\nu})'', \tag{3.2}$$

where $q^{\nu}=c(1+\varepsilon^{\nu}_{\kappa}\zeta)=qM_2$, $\kappa^{\nu}=\kappa M_2^2$, and $\varepsilon^{\nu}_{\kappa}=(1+\varepsilon_{\kappa})(M1/M2)-1$, where M_1 and M_2 are the molar masses of the components. This system of equations is, in fact, singular, since coefficients of the higher derivatives are proportional. Thus, we can derive one algebraic equation instead of a differential one,

$$\psi^{\nu}_0(c,\zeta) - \varepsilon^{\nu}_{\kappa}\mu^{\nu}_0(c,\zeta) = \psi^{\nu}_{\rm eq} - \varepsilon^{\nu}_{\kappa}\mu^{\nu}_{\rm eq}. \tag{3.3}$$

The bvp4c procedure takes only differential equations, so we have to transform Eq. (3.3) to a differential one. This can be done easily by taking the derivative of both sides. After some transformations, we have the following equation set:

$$(q^{\nu})'' = \frac{1}{\kappa^{\nu}}[\mu^{\nu}_0(c,\zeta) - \mu^{\nu}_{\rm eq}],$$

$$\zeta' = -(q^{\nu})'\left[(1+\varepsilon^{\nu}_{\kappa}\zeta)\frac{\psi^{\nu}_{0\zeta} - \varepsilon^{\nu}_{\kappa}\mu^{\nu}_{0\zeta}}{\psi^{\nu}_{0c} - \varepsilon^{\nu}_{\kappa}\mu^{\nu}_{0c}} - \frac{\varepsilon^{\nu}_{\kappa}q}{1+\varepsilon^{\nu}_{\kappa}\zeta}\right]^{-1}, \tag{3.4}$$

where subscripts ζ or c mean partial derivative of the corresponding quantity with respect to ζ or c. This is the system of 3 first-order differential equations for 3 variables ζ, q^{ν}, and $(q^{\nu})'$, which requires 3 boundary conditions. One of them is Eq. (3.3) taken on one of the boundaries, which simply determines the integration constant for the second differential equation. The other two are $(q^{\nu})'(x_g)=0$ and $(q^{\nu})'(x_{\ell})=0$, which indicates the fact that box boundaries are in the homogeneous region.

The numerical procedure allows the variables to take any value. However, not all the values are allowed physically. For instance, the mole fraction ζ is bounded in the interval $(0;1)$ and the molar concentration is bounded in the interval $(0;B^{-1})$, where B is given in Eq. (2.7). In order to avoid out-of-range problems, we use the function which safely maps a unit interval to real axes,

$$X(u) = \arcsin(2u-1) \quad \text{and } X'(u,u') \equiv \frac{d}{dx}X(u) = \frac{u'}{\sqrt{u-u^2}}. \tag{3.5}$$

Particularly, the actual variables, which we provide to the bvp4c procedure are

$$Y_1 = X(\zeta),$$

$$Y_2 = X(q^{\nu}/q^{\nu}_{\infty}),$$

$$Y_3 = X'[q^{\nu}/q^{\nu}_{\infty},(q^{\nu})'/q^{\nu}_{\infty}], \tag{3.6}$$

where $q^{\nu}_{\infty}=B^{-1}\max(1,|\varepsilon^{\nu}_{\kappa}|)$ is the limiting value for q^{ν}.

B. Nonequilibrium profile

Nonequilibrium conditions are implemented by changing temperature or pressure from their equilibrium values. This results in mass and heat fluxes through the interface. The amount of matter will then change in the gas and liquid phase. We will put the system in such conditions, that the total contents of the box is constant and equal to the equilibrium contents. It means that if some amount of liquid has been evaporated, the same amount of gas is condensed externally and put back into the liquid phase.

We introduce the overall mass $m(x)=\int_{x_g}^{x} dy\rho(y)$ and the mass of the first component $m_{\xi}(x)=\int_{x_g}^{x} dy\rho(y)\xi(y)$, which obey the following equations by definition:

$$m'(x) = \rho(x),$$

$$m'_{\xi}(x) = \rho(x)\xi(x). \tag{3.7}$$

We introduce the overall mass flux J_m, the mass flux of the first component J_{ξ}, the energy flux J_e, and the "pressure" flux J_p,

$$J_m = \rho \mathrm{v},$$

$$J_{\xi} = J_1 + \xi J_m,$$

$$J_e = J_q + J_m\left[u_0 + \frac{1}{2}\left(\frac{J_m}{\rho}\right)^2 + \frac{1}{\rho}\left(p_{\perp} - \frac{1}{2}\kappa q'^2\right) - gx\right],$$

$$J_p = p_{\perp} + \frac{J_m^2}{\rho} - mg. \tag{3.8}$$

From Sec. II A one can see that all these fluxes are constant.

From Eq. (2.11) we obtain

$$\kappa q'' = \frac{1}{q}\left(p_0 - p_{\perp} + \frac{1}{2}q'^2\right),$$

$$\kappa q'' = \frac{1}{\varepsilon_{\kappa}}(\psi_0 - \psi), \tag{3.9}$$

where $p_{\perp}(x)=p(x)+\kappa q'^2$. As in Eq. (3.2) we have a singular set which leads to the algebraic equation

$$\psi_0 - \psi - \frac{\varepsilon_{\kappa}}{q}\left(p_0 - p_{\perp} + \frac{1}{2}q'^2\right) = 0. \tag{3.10}$$

Taking derivative of this equation with respect to the coordinate we obtain the expression for the first derivative of the fraction

$$\xi' = \frac{\psi' - [\,\psi_0|'_{\xi} - (p_0 - p_{\perp})|'_{\xi}(\varepsilon_{\kappa}/q)]}{\psi_{0\xi} - (p_0 - p_{\perp})_{\xi}(\varepsilon_{\kappa}q)}, \tag{3.11}$$

where $\varphi_{\xi} \equiv (\partial\varphi/\partial\xi)$ and $\varphi|'_{\xi} \equiv \varphi' - \varphi_{\xi}\xi' = \varphi_q q' + \varphi_T T'$ for any φ. The expressions for ψ', T', and q' are taken from Eq.

TABLE I. The molar mass and the van der Waals coefficients of cyclohexane (1) and hexane (2).

Component	$M\times10^{-3}$ (kg/mol)	a (J m^3/mol^2)	$b\times10^{-5}$ (m^3/mol)
1	84.162	2.195	14.13
2	86.178	2.495	17.52

(2.15) and Eq. (3.9). The expressions for p_0, ψ_0, as well as ψ_{0T}, ψ_{0q}, and $\psi_{0\xi}$ one can derive from Eq. (2.5) using standard formulas. Furthermore, $p_{\perp\xi}=-J_m^2\varepsilon_\kappa/q$ and $p_\perp|'_\xi=(qg+q'J_m^2/q^2)/(1+\varepsilon_\kappa\xi)$.

As a consequence we have 7 unknown variables, q, q', m, m_ξ, ξ, T, ψ, and 4 unknown fluxes, J_m, J_ξ, J_e, J_p. This requires 7 first-order differential equations and 11 boundary conditions (7 of them determine integration constants of differential equations and 4 of them determine constant fluxes). As differential equations we use Eq. (3.7), Eq. (2.15), one of Eq. (3.9), and Eq. (3.11). As boundary conditions we use the following: The first boundary condition is Eq. (3.10) taken on one of the boundaries, which simply determine the integration constant for Eq. (3.11). The 4 other conditions control the overall content of the box (particularly, it is the same as in equilibrium),

$$m(x_g)=0,$$

$$m_\xi(x_g)=0,$$

$$m(x_\ell)=m_{\rm eq},$$

$$m_\xi(x_\ell)=m_{\xi,\rm eq}. \tag{3.12}$$

Here $m_{\rm eq}$ and $m_{\xi,\rm eq}$ are the equilibrium values of the total overall mass and the total mass of the first component in the whole box. The 2 more conditions are

$$q'(x_g)=0,$$

$$q'(x_\ell)=0, \tag{3.13}$$

which indicate the fact that box boundaries are in the homogeneous region. In contrast to the equilibrium case, the density in the nonequilibrium homogeneous region may vary with coordinate, so q' differs from zero on the boundaries, and, in fact, they do. The value of the q' is, however, small in the homogeneous region, comparing to the value in the surface region, so we may neglect it and use such approximation. This will lead to the wrong profile behavior only in the small vicinity on the boundary, which we will exclude from the further analysis. The choice of the 4 last boundary conditions should preferably reflect the conditions of a possible experiment. For instance, we may control the temperatures on both sides of the box, the pressure on the vapor side and the fraction on the liquid side,

$$T(x_g)=T^g,$$

$$T(x_\ell)=T^\ell,$$

$$p_\perp(x_g)=p^g,$$

$$\xi(x_\ell)=\xi^\ell. \tag{3.14}$$

To solve these equations numerically we use the same techniques as in the equilibrium case. All the variables should be properly scaled in order to make them the same order of magnitude. This balances the numerical residual and gives better solution result. We use the following variables:

$$Y_1=X(\xi),$$

$$Y_2=X(q/q_\infty),$$

$$Y_3=X'(q/q_\infty,q'/q_\infty),$$

$$Y_4=m/(x^*q^*),$$

$$Y_5=m_\xi/(x^*q^*),$$

$$Y_6=T^*/T,$$

$$Y_7=(\psi/T)(T^*/\psi^*), \tag{3.15}$$

where X is defined in Eq. (3.5), $q_\infty=q_\infty^\nu/M_2$, and scaling parameters $x^*=x_\ell-x_g$, $T^*=T_{\rm eq}$, $\psi^*=\psi_{\rm eq}$, $q^*=p_{\rm eq}/\psi_{\rm eq}$.

TABLE II. Transport coefficients.

Phase and/or component	λ [W/(m K)] 1	2	D (m^2/s)	s_T (1/K)
Gas	0.0140	0.0157	3.876×10^{-5}	10^{-4}
Liquid	0.1130	0.1090	3.876×10^{-9}	10^{-4}

IV. TEMPERATURE AND CHEMICAL POTENTIAL PROFILES

A. Data input

In this section we show some profiles, obtained with the help of the above procedure. We choose a mixture of cyclohexane (component 1) and n-hexane (component 2) and give some of their properties relevant for our calculation in the table below. We note that among them only the molar masses have been measured. There are a number of problems to obtain the values of other material properties. We determined, for instance, the two van der Waals coefficients of the pure phases using their critical temperatures and pressures.[2] As a consequence the critical volumes per mole found in our description for the pure components differs substantially from the experimental value. For the mixture the van der Waals coefficients were then found using the mixing rules, Eq. (2.7). We use the values of the molar mass and the van der Waals coefficients given in Table I.

[2]In this we follow the example of the *Handbook of Chemistry and Physics* [23] rather than Refs. [11,21] where T_c and v_c were used.

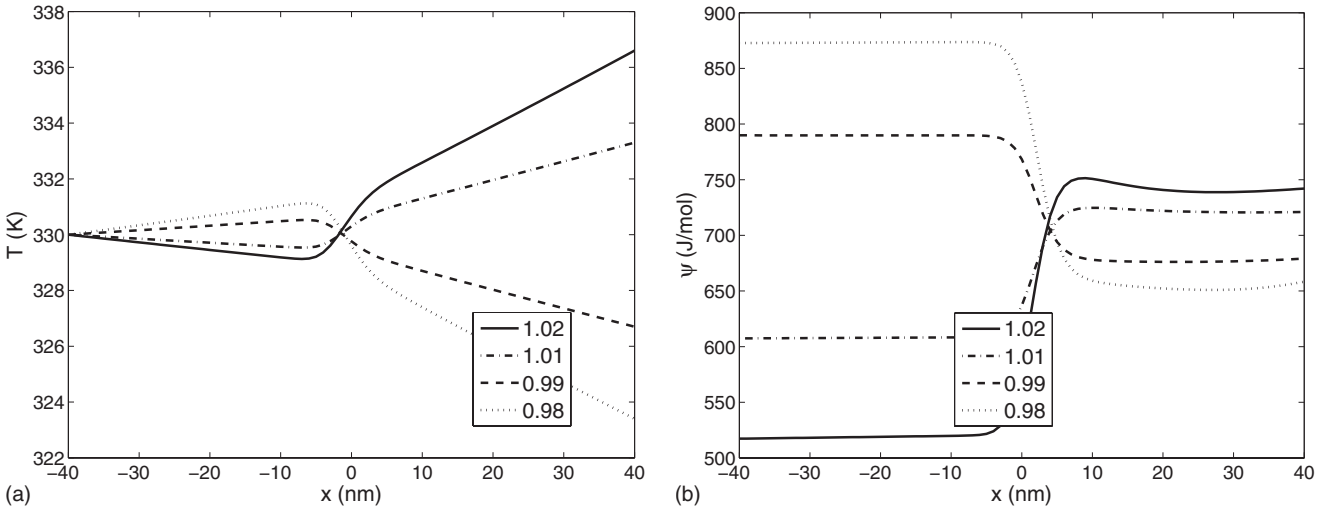

FIG. 1. Temperature and chemical potential difference profiles at various T^{ℓ}.

Transport coefficients of homogeneous fluids depend on temperature and densities, while these dependencies are not always available. We use typical constant values of these coefficients at the conditions, close to the above equilibrium conditions. The values of the thermal conductivity λ are well tabulated and we take them from [24]. We take a typical value of the diffusion coefficient D for a liquid mixture in the barycentric frame of reference from [25] and use the argument from Ref. [20], p. 279, to obtain the typical value of the diffusion coefficient for a gas mixture. Another argument from [20], p. 279 is used to obtain the typical value of the Soret coefficient s_T. We use the data given in Table II together with the "mixing" rules for the heat conductivity

$$\lambda^g = \xi^q_{\rm eq}\lambda^g_1 + (1-\xi^q_{\rm eq})\lambda^g_2,$$

$$\lambda^{\ell} = \xi^{\ell}_{\rm eq}\lambda^{\ell}_1 + (1-\xi^{\ell}_{\rm eq})\lambda^{\ell}_2. \tag{4.1}$$

In the calculations in this paper we took the term related to the possibility of excess resistivities in the interfacial region equal to zero, $\alpha_{qq}=0$, $\alpha_{q1}=0$, and $\alpha_{11}=0$ in Eq. (2.16). As one can see in the figures in [1] the choice of $\alpha_{qq}=1$ of $\alpha_{11}=1$ leads to a relatively minor change in the continuous profiles. In view of the complexity of the analysis we therefore restricted the analysis to zero α's. We do not expect finite and realistic values of α's will modify our results regarding the validity of local equilibrium for the surface.

The values of the gradient coefficients are not available at all. One can determine them comparing the actual value of the surface tension of a pure fluid with the one, calculated with a given $\kappa_{\rho_i\rho_j}$. For given conditions the value of the surface tension of the mixture is about 0.027 N/m. We therefore choose κ^{ν} to be equal to 12×10^{-18} J m^5/mol^2 and $\varepsilon^{\nu}_{\kappa}=0.01$. This gives $\kappa\simeq16\times10^{-16}$ J m^5/kg^2 and $\varepsilon_{\kappa}\simeq0.03$ according to the line below Eq. (3.2). This also gives values of the surface tension around 0.03 N/m.

B. Results

The equilibrium properties of the system are calculated[3] at $T_{\rm eq}=330$ K and $\psi^{\nu}_{\rm eq}=700$ J/mol. This gives $p_{\rm eq}=376\,095$ Pa, $\mu^{\nu}_{\rm eq}=-57\,098$ J/mol, $c^g_{\rm eq}=153.23$ mol/m^3, $c^{\ell}_{\rm eq}=4898.26$ mol/m^3, $\zeta^g_{\rm eq}=0.5519$, and $\zeta^{\ell}_{\rm eq}=0.5934$.

The mixture is then perturbed from equilibrium for the following three cases: (1) setting T^{ℓ} equal to 0.98, 0.99, 1.01, 1.02 of $T_{\rm eq}$ and keeping T^g, p^g, and ζ^{ℓ} equal to their equilibrium values, see Fig. 1; (2) setting p^g equal to 0.98, 0.99, 1.01, 1.02 of $p_{\rm eq}$ and keeping T^g, T^{ℓ}, and ζ^{ℓ} equal to their equilibrium values, see Fig. 2; (3) setting ζ^{ℓ} equal to 0.98, 0.99, 1.01, 1.02 of $\zeta^{\ell}_{\rm eq}$ and keeping T^g, T^{ℓ}, and p^g equal to their equilibrium values, see Fig. 3. Both the profiles and the equilibrium properties were calculated with an accuracy 10^{-6}.

V. LOCAL EQUILIBRIUM OF THE SURFACE

In equilibrium it is possible to describe the surface in terms of Gibbs excess quantities [3]. One can treat a system of coexisting liquid and vapor as a three-phase system: liquid and vapor bulk phases and the surface. The surface has thermodynamic properties. The temperature and chemical potentials have the same equilibrium value as in the rest of the system. Furthermore the thermodynamic state of the surface is given by excess concentrations and thermodynamic potentials. Following Gibbs we have for the surface

$$h^s_{\rm eq} = \mu_{1,\rm eq}c^s_{1,\rm eq} + \mu_{2,\rm eq}c^s_{2,\rm eq} + T_{\rm eq}s^s_{\rm eq},$$

$$u^s_{\rm eq} = \mu_{1,\rm eq}c^s_{1,\rm eq} + \mu_{2,\rm eq}c^s_{2,\rm eq} + \gamma^s_{\rm eq} + T_{\rm eq}s^s_{\rm eq},$$

$$f^s_{\rm eq} = \mu_{1,\rm eq}c^s_{1,\rm eq} + \mu_{2,\rm eq}c^s_{2,\rm eq} + \gamma^s_{\rm eq},$$

[3]From now on we will use specific quantities per unit of mole in the description. We will omit the superscript ν in the following sections.

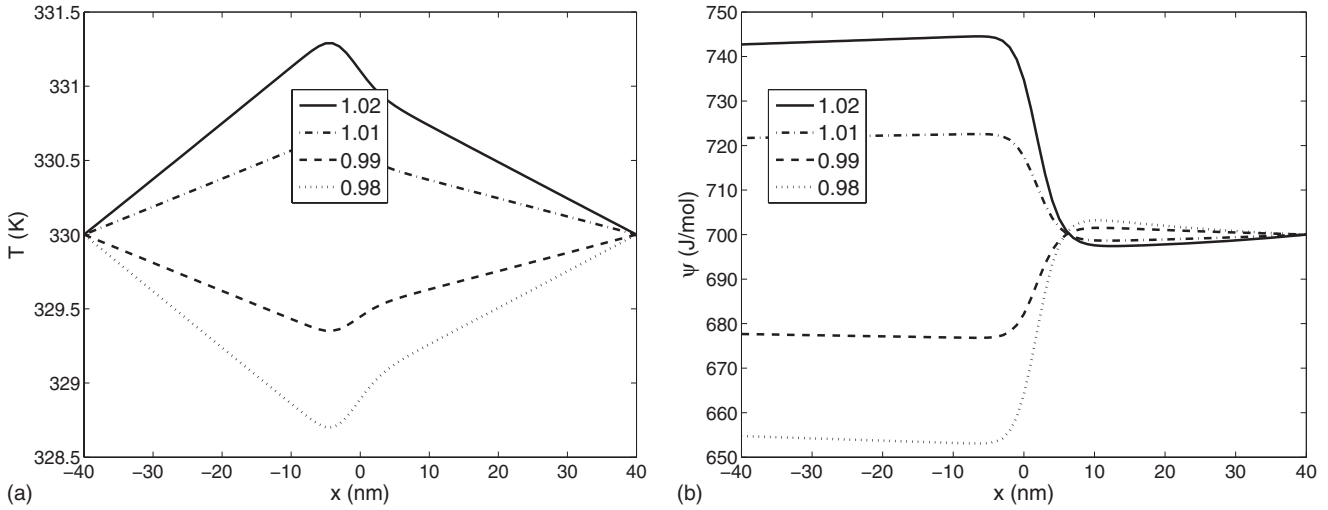

FIG. 2. Temperature and chemical potential difference profiles at various p^g.

$$g^s_{\rm eq} = \mu_{1,\rm eq} c^s_{1,\rm eq} + \mu_{2,\rm eq} c^s_{2,\rm eq}. \tag{5.1}$$

The superscript s indicates here the surface and equal to the excess of corresponding quantities. In these relations the equilibrium temperature and chemical potentials are the same everywhere independent of the choice of the dividing surface. The excesses depend on the choice of the dividing surface, in a such way that the above relations are true for any choice of the dividing surface, see Gibbs [3].

It is our aim in this paper to show that the surface in a nonequilibrium liquid-vapor system can also be described as a separate thermodynamic phase using the Gibbs excess quantities. We will call this property local equilibrium of the surface. The property of local equilibrium for the surface implies that it is possible to define all thermodynamic properties of a surface such that they have their equilibrium coexistence values for any choice of the dividing surface given the temperature of the surface T^s and the chemical potential difference $\psi^s \equiv \mu^s_1 - \mu^s_2$. For this purpose we will define the excess densities in Sec. V A. Furthermore we will in Sec. V B develop a method to obtain T^s and ψ^s which are independent of the choice of the dividing surface. The procedure both in Sec. V A and Sec. V B uses the numerical solution of the system in stationary nonequilibrium states. In the rest of the paper we discuss the precise meaning of local equilibrium, verify its validity and in the process verify that the surface temperature and chemical potential difference are indeed independent of the choice of the dividing surface.

A. Defining the excess densities

The definition of the excesses consists of 3 steps: determining the phase boundaries, defining the specified dividing surface and, in particular, defining the excesses.

To determine the phase boundaries we will use the order parameter q. We introduce a small parameter β and define the β-dependent boundary, $x^{g,s}_\beta$, between the vapor and the surface by

$$\left| \frac{q(x^{g,s}_\beta) - q_{eos}(p_\perp(x^{g,s}_\beta), \xi(x^{g,s}_\beta), T(x^{g,s}_\beta))}{q(x^{g,s}_\beta)} \right| \equiv \beta, \tag{5.2}$$

where $q_{eos}(p_\perp, \xi, T)$ is the equation of state's value (no gradient contributions) of q for pressure $p_\perp$, mass fraction ξ, and temperature T. The β-dependent boundary, $x^{\ell,s}_\beta$, between the surface and the liquid is defined in the same way.

The numerical procedure calculates profiles only at specified grid points, which we provide to the procedure. That means that $x^{g,s}_\beta$ and $x^{\ell,s}_\beta$ can only be situated at points of the grid. We choose their position to be the last bulk point of the grid where the left-hand side of Eq. (5.2) does not exceed the right-hand side. In our calculations we will choose $\beta = 10^{-3}$ and use a grid of 81 points.

We shall also choose bulk boundaries near the box boundary where, because of the finite size of the box, the behavior of the profiles might be uncharacteristic. To avoid this effect, we do not consider the first 5 points of each phase close to these boundaries when we calculate the properties in these phases. The 6th point we call x^g and the 76th point x^ℓ.

The bulk gas therefore ranges from x^g to $x^{g,s}_\beta$ and the bulk liquid ranges from $x^{\ell,s}_\beta$ to x^ℓ. The surface therefore ranges from $x^{g,s}_\beta$ to $x^{\ell,s}_\beta$. In order to define excess quantities properly we always choose conditions such that the widths of the vapor and the liquid phases $x^{g,s}_\beta - x^g$ and $x^\ell - x^{\ell,s}_\beta$ are larger then the surface width $x^{\ell,s}_\beta - x^{g,s}_\beta$.

In order to determine excess densities we need to extrapolate profiles from the vapor and the liquid phases into the interfacial region. In equilibrium extrapolated bulk profiles are constants which are equal to the coexisting values of the corresponding quantities. Nonequilibrium bulk profiles are not constant. We fit the bulk profile with a polynomial of order $n_b = 2$ and use this polynomial to extrapolate nonequilibrium bulk profiles into the interfacial region. This is done with the help of MATLAB functions `polyfit` and `polyval`. The extrapolation of the bulk profiles introduces a certain error depending on the choice of β and n_b in particular for nonequilibrium systems. This error is the main source of

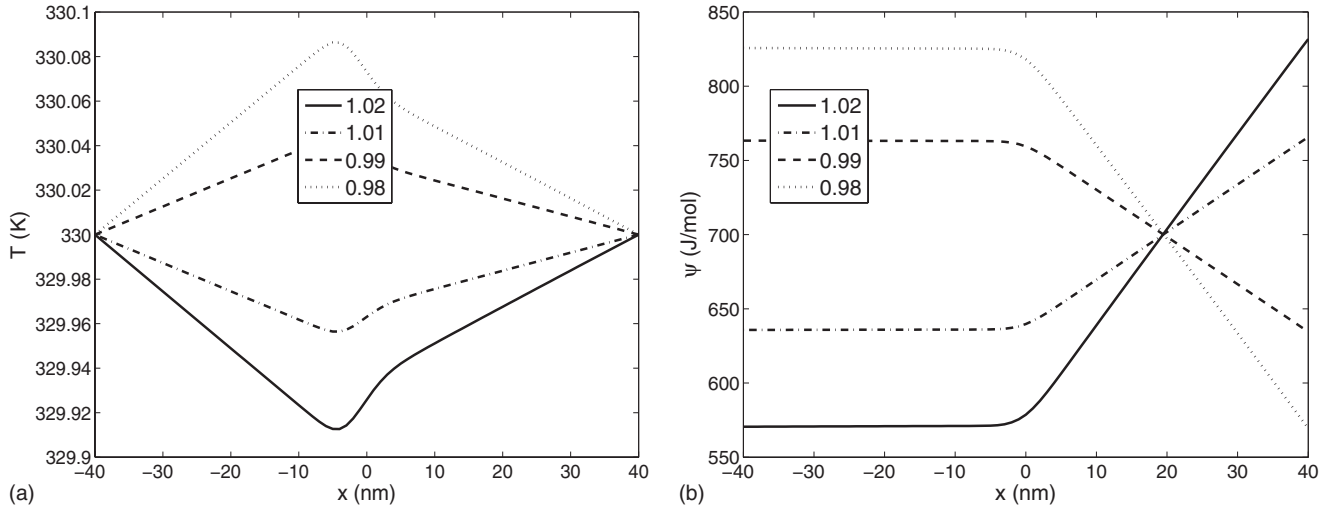

FIG. 3. Temperature and chemical potential difference profiles at various ζ^{ℓ}.

inaccuracy in the determination of the surface quantities. We will come back to this later.

The distances between commonly used dividing surfaces, such as for instance the equimolar surface and the surface of tension, are very small [2,11]. Thus, if there occurs an error in the determination of a dividing surface using a course grid, it would lead to inaccurate results. We therefore divide each interval of the course grid between $x_\beta^{g,s}$ and $x_\beta^{\ell,s}$ in 10^4 subintervals. This surface grid is used for all operations related to the surface. Within the interfacial region we interpolate all the profiles (which were obtained by extrapolation from the bulk to the surface region using the course grid) from the course grid to the surface grid using a polynomial of order $n_s=3$ with the help of MATLAB functions `polyfit` and `polyval`.

We can now define the excess $\hat{\phi}$ of any density $\phi(x)$ as a function of a dividing surface x^s as

$$\hat{\phi}(x^s) = \int_{x_\beta^{g,s}}^{x_\beta^{\ell,s}} dx[\phi(x) - \phi^g(x)\Theta(x^s - x) - \phi^\ell(x)\Theta(x - x^s)], \tag{5.3}$$

where ϕ^g and ϕ^ℓ are the extrapolated gas and liquid profiles and $\Theta(t)$ is the Heaviside function. The density ϕ is per unit of volume and $\hat{\phi}$ is per unit of surface area. In our calculations integration is performed using the trapezoidal method by MATLAB function trapz.

We can now define different dividing surfaces. The equimolar dividing surface x^c is defined by the equation $\hat{c}(x^c)=0$. Analogously, we define equimolar surfaces with respect to component 1 and 2: $\hat{c}_1(x^{c_1})=0$ and $\hat{c}_2(x^{c_2})=0$, and the equidensity surface x^ρ. The surface of tension x^γ is defined from the equation $x^\gamma \hat{p}_\parallel(x^\gamma) - \hat{xp}_\parallel(x^\gamma)=0$. All the densities are given as arrays on a coordinate grid, but not as continuous functions. Thus, in order to find the solution of an equation $\varphi(x)=0$ we calculate the values $\varphi_i=\varphi(x_i)$ for each point x_i within the surface region and find the minimum of its absolute value, $\min_i(|\varphi_i|)$. Because of the discrete nature of the argument this value may not be equal to zero, but it will be the closest to zero among all other coordinate points. So we will call this point the root of the equation $\varphi(x)=0$. We use the fine surface grid in this procedure.

If follows from Eq. (5.3) that

$$\frac{d\hat{\phi}(x_s)}{dx_s} = \phi^\ell(x_s) - \phi^g(x_s), \tag{5.4}$$

which we will use later.

B. Defining the temperature and chemical potential difference

An equilibrium two-phase two-component mixture has two free parameters, for instance the temperature T and the chemical potential difference $\psi=\mu_1-\mu_2$. *Local equilibrium of a surface* implies that also in nonequilibrium it should be possible to define the temperature T^s and the chemical potential difference ψ^s of the surface. As found in Ref. [11] for the surface temperature in the one-component system, both T^s

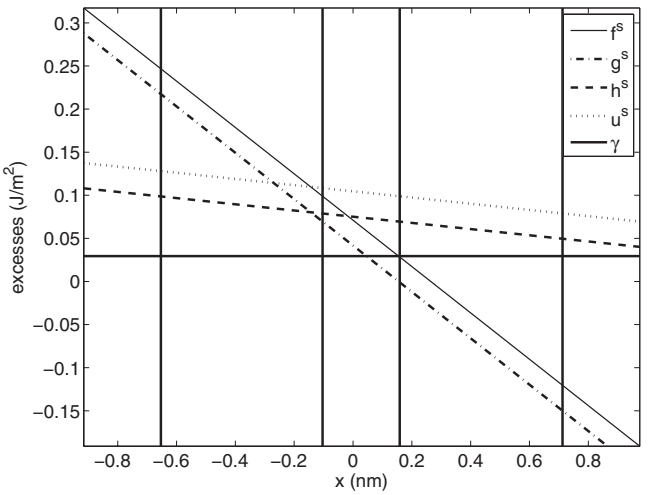

FIG. 4. Equilibrium excesses at $T=330$ K and $\psi=700$ J/mol as functions of the position of the dividing surface. The vertical lines indicate the x^{c_2}, x^γ, x^c, x^{c_1} dividing surfaces from left to right.

and ψ^s should be independent of the choice of the dividing surface.

The equilibrium temperature and chemical potential difference determine all other equilibrium properties of the surface. Thus, there is a bijection from $T_{\rm eq}$ and $\psi_{\rm eq}$ to any other set of independent excess variables $X_{1,\rm eq}$ and $X_{2,\rm eq}$, so that one can use them equally well in order to characterize a surface. In nonequilibrium the temperature and chemical potential difference vary through the interfacial region, but as $X_{1,ne}$ and $X_{2,ne}$ are excesses, they characterize the whole surface. If a nonequilibrium surface is in local equilibrium, the same bijection should exist. This implies that given two independent nonequilibrium excesses $X_{1,ne}$ and $X_{2,ne}$ one can determine the temperature T^s and the chemical potential ψ^s of the whole surface. Thus one can calculate equilibrium tables of $X_{1,\rm eq}(T_{\rm eq},\psi_{\rm eq})$ and $X_{2,\rm eq}(T_{\rm eq},\psi_{\rm eq})$ for different values of $T_{\rm eq}$ and $\psi_{\rm eq}$ and then determine temperature and chemical potential of a surface as $T^s=T_{\rm eq}(X_{1,ne},X_{2,ne})$ and $\psi^s=\psi_{\rm eq}(X_{1,ne},X_{2,ne})$.

As we want the temperature and chemical potential difference to be independent of the position of the dividing surface, we shall use excesses which are also independent of the position of a dividing surface in equilibrium for X_1 and X_2. For two component mixtures these independent variables are the surface tension γ and the relative adsorption Γ_{12}. If the number of components is more than 2, additional relative adsorptions should be used.

These quantities are well defined for equilibrium, but not for nonequilibrium. So we will define them first. In equilibrium the surface tension is defined as minus the excess of the parallel pressure $\gamma_{\rm eq}=-\hat{p}_\parallel$. Alternatively one often uses the integral of $p_\perp-p_\parallel(x)\equiv\gamma_{xx}(x)$ across the interface: $\gamma_{\rm eq}=\int dx\,\gamma_{xx}(x)$. Both definitions are equivalent in equilibrium since $p_\perp$ is constant through the interface and $\gamma_{xx}(x)$ is identically zero in the bulk phases. In nonequilibrium $\gamma_{xx}(x)$ may differ from zero in the bulk regions, however, and this makes the second definition inappropriate. We will therefore define the nonequilibrium surface tension using the standard definition [11]

$$\gamma(x^s)=-\hat{p}_\parallel(x^s). \tag{5.5}$$

This quantity differs from $\hat{\gamma}_{xx}$ by the term equal to $\hat{p}_\perp$, which is usually small compared to $\hat{p}_\parallel$.

The relative adsorption is defined as $\Gamma_{12,\rm eq}=\hat{c}_{1,\rm eq}-\hat{c}_{2,\rm eq}(c^\ell_{1,\rm eq}-c^g_{1,\rm eq})/(c^\ell_{2,\rm eq}-c^g_{2,\rm eq})$ in equilibrium [6], where $c^\ell_{i,\rm eq}$ and $c^g_{i,\rm eq}$ are coexistence concentrations of the corresponding components. Since these quantities are not constant in nonequilibrium, we cannot use this definition directly. One can however see from Eq. (5.4) that both in equilibrium and nonequilibrium $\hat{c}_i'(x^s)=c^\ell_i(x^s)-c^g_i(x^s)$, where the prime indicates a spatial derivative. Since in equilibrium $c^\ell_i(x^s)-c^g_i(x^s)=c^\ell_{i,\rm eq}-c^g_{i,\rm eq}$ we can use the following definition:

$$\Gamma_{12}(x^s)=\hat{c}_1(x^s)-\hat{c}_2(x^s)\frac{c^\ell_1(x^s)-c^g_1(x^s)}{c^\ell_2(x^s)-c^g_2(x^s)}, \tag{5.6}$$

both in equilibrium and nonequilibrium.

If the system is in local equilibrium we may write

$$\gamma(x^s)=\gamma_{\rm eq}(T^s,\psi^s),$$

$$\Gamma_{12}(x^s)=\hat{c}_1(x^s)-\hat{c}_2(x^s)\frac{c^\ell_{1,\rm eq}(T^s,\psi^s)-c^g_{1,\rm eq}(T^s,\psi^s)}{c^\ell_{2,\rm eq}(T^s,\psi^s)-c^g_{2,\rm eq}(T^s,\psi^s)}. \tag{5.7}$$

Substituting the expressions for $\gamma(x_s)$ and $\Gamma_{12}(x_s)$ from Eq. (5.5) and Eq. (5.6) into Eq. (5.7) we obtain the following relations:

$$\hat{p}_\parallel(x^s)=\hat{p}_{\parallel,\rm eq}(T^s,\psi^s),$$

$$\frac{c^\ell_1(x^s)-c^g_1(x^s)}{c^\ell_2(x^s)-c^g_2(x^s)}=\frac{c^\ell_{1,\rm eq}(T^s,\psi^s)-c^g_{1,\rm eq}(T^s,\psi^s)}{c^\ell_{2,\rm eq}(T^s,\psi^s)-c^g_{2,\rm eq}(T^s,\psi^s)}. \tag{5.8}$$

This gives the bijection equations to determine T^s and ψ^s from the actual nonequilibrium variables. As the left-hand sides in Eq. (5.8) are in good approximation independent of the position of the dividing surface, T^s and ψ^s are similarly independent on this position.

C. Defining local equilibrium

The other quantities required for the Gibbs description of the nonequilibrium surfaces we define in the following way. The surface chemical potentials are the equilibrium coexistence values determined via the procedure discussed in Sec. III A,

$$\mu^s_1\equiv\mu_{1,\rm eq}(T^s,\psi^s),$$

$$\mu^s_2\equiv\mu_{2,\rm eq}(T^s,\psi^s). \tag{5.9}$$

We define the surface extensive properties as[4]

$$\phi^s(x^s)\equiv\hat{\phi}(x^s) \tag{5.10}$$

The local equilibrium of a surface should be established for any choice of a dividing surface. The results of the calculations for any particular choice of a dividing surface may not be representative since they differ for another choice of a dividing surface. Thus, the property of local equilibrium should be established for all dividing surfaces together.

Consider the profile of an excess $\hat{\phi}(x^s)$ as a function of position of a dividing surface x^s. It follows from Eq. (5.4) that the slope of the excess profile is equal to the difference between the extrapolated values of a profile of thermodynamic quantity ϕ. In equilibrium these values are constant and equal to the coexistence values. Thus, equilibrium excess densities are linear functions of the position of the dividing surface, as one can see on Fig. 4. Nonequilibrium profiles in the bulk phases are not constant. We construct the extrapolated profiles using n_bth order polynomials with $n_b=2$. Resulting nonequilibrium excesses are therefore polynomials of the order $n_b+1=3$, according to Eq. (5.4). These excesses, for the most extreme case of nonequilibrium perturbation $T^\ell=1.02T_{\rm eq}$, are shown in Fig. 5. Even though these excesses are polynomials of the third order they are very close to straight lines. As one can see from Fig. 6 the variation in the slope is about 1% through the whole surface. It indicates that

[4]Note that for some quantities this definition differs from the one used in [11]. We will come back to this point later.

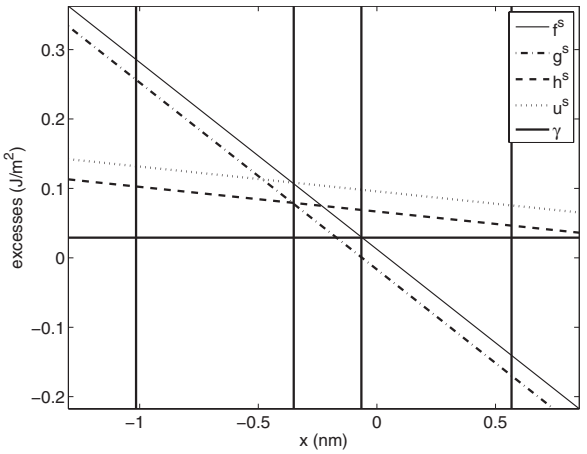

FIG. 5. Nonequilibrium excesses for the case of perturbing $T^{\ell}=1.02T_{\mathrm{eq}}$ as functions of the position of the dividing surface. The vertical lines indicate the x^{c2}, x^{γ}, x^{c}, x^{c1} dividing surfaces from left to right.

this nonequilibrium "state" is very close to an equilibrium one.

We therefore develop the procedure to relate the nonequilibrium state to an equilibrium one by comparing thermodynamic quantities in equilibrium and in nonequilibrium. The comparison performed in one particular point of the surface may not be sufficient because it may suffer from artifacts peculiar to this particular surface. Moreover, any comparison performed in a particular point does not speak for the whole. We therefore compare the nonequilibrium surface with an equilibrium one for all dividing surfaces together. We will use the least square sum method for this.

Consider a nonequilibrium thermodynamic excess $t^s(x^s)$ and a quantity $r^s(x^s;T,\psi)$ which is a combination of excesses and may depend on (T,ψ) as parameters. We introduce the following measures of the difference of t^s and r^s:

$$\delta_{t^s,r^s}(x^s;T,\psi)\equiv\left|t^s(x_i^s)-r^s(x_i^s;T,\psi)\right| \tag{5.11}$$

and

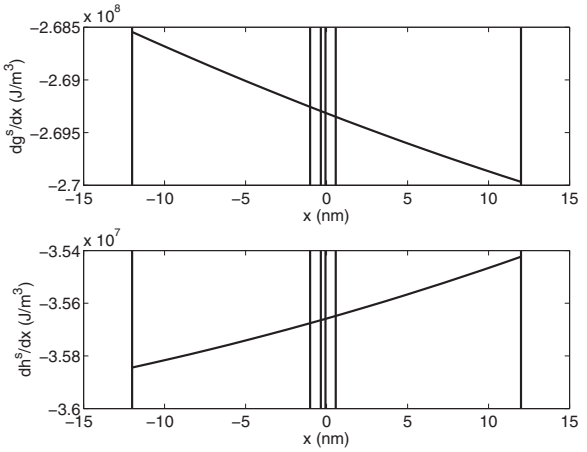

FIG. 6. Slopes of nonequilibrium excesses for the case of perturbing $T^{\ell}=1.02T_{\mathrm{eq}}$ as functions of the position of the dividing surface. The vertical lines indicate the surface boundaries and x^{c2}, x^{γ}, x^{c}, x^{c1} dividing surfaces.

$$S_{t^s,r^s}(T,\psi)\equiv\sum_{i\in\mathrm{surface}}\left[t^s(x_i^s)-r^s(x_i^s;T,\psi)\right]^2,$$

$$\sigma_{t^s,r^s}(T,\psi)\equiv\frac{1}{N}\sqrt{S_{t^s,r^s}(T,\psi)}, \tag{5.12}$$

where N is the number of surface points.

We say that t^s and r^s are *the same* in the surface if the value of $\sigma_{t^s,r^s}(T,\psi)$ is negligible compared to the typical value of either $|t^s(x^s)|$ or $|r^s(x^s;T,\psi)|$. If two quantities t^s and r^s are the same in the above sense, we say that the nonequilibrium state of the surface is characterized by surface temperature $T^s_{\{x^s\}}$ and chemical potential difference $\psi^s_{\{x^s\}}$ if

$$S_{t^s,r^s}(T^s_{\{x^s\}},\psi^s_{\{x^s\}})=\min_{T,\psi}S_{t^s,r^s}(T,\psi). \tag{5.13}$$

Here superscript s indicates that we speak about surface quantities only (as everywhere in this paper) and subscript $\{x^s\}$ indicates that $T^s_{\{x^s\}}$ and $\psi^s_{\{x^s\}}$ are the parameters for all dividing surfaces together [in contrast to the values $T^s(x^s)$ and $\psi^s(x^s)$ determined from Eq. (5.8) for each particular dividing surface x^s].

These definitions are easy to illustrate in equilibrium. For instance, for $h^s_{\mathrm{eq,gibbs}}(x^s;T,\psi)\equiv\mu_{1,\mathrm{eq}}(T,\psi)c^s_{1,\mathrm{eq}}+\mu_{2,\mathrm{eq}}(T,\psi)c^s_{2,\mathrm{eq}}+Ts^s_{\mathrm{eq}}$ it follows from Eq. (5.1) that $h^s_{\mathrm{eq}}(x^s;T_{\mathrm{eq}},\psi_{\mathrm{eq}})=h^s_{\mathrm{eq,gibbs}}(x^s;T_{\mathrm{eq}},\psi_{\mathrm{eq}})$. Furthermore $g^s_{\mathrm{eq}}(x^s;T_{\mathrm{eq}},\psi_{\mathrm{eq}})\neq h^s_{\mathrm{eq,gibbs}}(x^s;T_{\mathrm{eq}},\psi_{\mathrm{eq}})$. Thus $\delta_{h^s_{\mathrm{eq}},h^s_{\mathrm{eq,gibbs}}}(x^s;T_{\mathrm{eq}},\psi_{\mathrm{eq}})=0$ and $\delta_{g^s_{\mathrm{eq}},h^s_{\mathrm{eq,gibbs}}}(x^s;T_{\mathrm{eq}},\psi_{\mathrm{eq}})\neq 0$. It is also true that $S_{h^s_{\mathrm{eq}},h^s_{\mathrm{eq,gibbs}}}(T_{\mathrm{eq}},\psi_{\mathrm{eq}})=\min S_{h^s_{\mathrm{eq}},h^s_{\mathrm{eq,gibbs}}}(T,\psi)$ and $\sigma_{h^s_{\mathrm{eq}},h^s_{\mathrm{eq,gibbs}}}(T,\psi)\leqslant\sigma_{g^s_{\mathrm{eq}},h^s_{\mathrm{eq,gibbs}}}(T,\psi)$. According to the above definitions (i) $h^s_{\mathrm{eq,gibbs}}$ and h^s_{eq} are the same quantities, but $h^s_{\mathrm{eq,gibbs}}$ and g^s_{eq} are not the same; (ii) the equilibrium state is characterized by $(T_{\mathrm{eq}},\psi_{\mathrm{eq}})$; as it should be. While this analysis is trivial in equilibrium, it is not trivial in nonequilibrium.

Note that while in equilibrium the conditions $\delta_{t,r}(x^s;T_{\mathrm{eq}},\psi_{\mathrm{eq}})=0$ and $S_{t,r}(T_{\mathrm{eq}},\psi_{\mathrm{eq}})=\min S_{t,t}(T,\psi)$ are equivalent, in general it does not follow in nonequilibrium from Eq. (5.13) that

$$\delta_{t,r}(x^s;T,\psi)=0\quad\forall\,x^s. \tag{5.14}$$

Thus Eq. (5.14) is not a good measure of the equality of the quantities and states in nonequilibrium. We may therefore speak about the equality of thermodynamic quantities as well as about the state T^s and $\psi^s=\mu^s_1-\mu^s_2$ of the surface in nonequilibrium only in the least square sense, as it is given in Eq. (5.13).

Within establishing the local equilibrium property of a nonequilibrium surface we would like to verify the following properties: (i) the existence of the unique temperature T^s and chemical potential difference ψ^s of a nonequilibrium surface; (ii) the validity of Eq. (5.1) in nonequilibrium at the surface's T^s and ψ^s; (iii) the possibility to determine all the properties of a nonequilibrium surface from equilibrium tables at the surface's T^s and ψ^s. We do this in the following section.

VI. VERIFICATION OF LOCAL EQUILIBRIUM

We calculate the equilibrium properties (coexistence data, such as the pressure or bulk densities, as well as various excesses) of the system for the range of temperatures $T=\{325,326,\ldots,340\}$ K and the range of chemical potential differences $\psi=\mu_1-\mu_2=\{400,450,\ldots,1000\}$ J/mol. The value of a thermodynamic quantity at any point (T,ψ), which is between these is interpolated using the MATLAB procedures `interp2` and `griddata`.

The temperature range was chosen to be well above the triple point of both components (279.5 K and 177.9 K for cyclohexane and hexane, respectively) and below the critical temperature of both components (553.5 K and 507.5, respectively). As discussed in Sec. IV B the equilibrium mole fractions of cyclohexane in the vapor and in the liquid were 0.55 and 0.59, respectively, when the temperature was 330 K and the chemical potential difference was 700 J/mol. As one can see in Figs. 1–3 it was enough to consider the range of temperatures of 15 K and the range of chemical potential differences of 600 J/mol, for the stationary state conditions considered in this paper. A larger range would be necessary to consider for unrealistically extreme nonequilibrium conditions across the system.

A. Surface temperature and chemical potential difference

As was mentioned, in equilibrium both γ and Γ_{12} are independent of the location of the dividing surface x^s. Given the above definitions, Eq. (5.5) and Eq. (5.6), we can calculate these quantities for nonequilibrium states. Calculations show that even though γ and Γ_{12} are not exactly independent on x^s away from equilibrium, the relative deviation is so small (about 0.004% for γ and 4% for Γ_{12} in the worst case), that one can consider these quantities to be independent of the position of the dividing surface. Thus one may use them in order to find the temperature, T^s, and the chemical potential difference, ψ^s, of the surface in nonequilibrium states, which will be independent of the position of the dividing surface.

Using Eq. (5.12) and Eq. (5.8) together with Eq. (5.4) we construct the following expressions:

$$S_\gamma(T,\psi)=\sum_{x^s}[\hat{p}_\parallel(x^s)-\hat{p}_{\parallel,\mathrm{eq}}(T,\psi)]^2,$$

TABLE III. Surface temperatures (K) and chemical potential differences (J/mol) for the case of perturbing T^ℓ.

	$T^\ell=1.02T_{\mathrm{eq}}$		$T^\ell=0.98T_{\mathrm{eq}}$	
Surface	T^s	ψ^s	T^s	ψ^s
$\{x^s\}$	331.831	770.53	328.129	650.92
x^c	331.823	769.51	328.124	650.29
x^γ	331.828	770.22	328.123	650.21
x^{c_1}	331.814	767.97	328.127	650.43
x^{c_2}	331.838	771.86	328.121	650.1

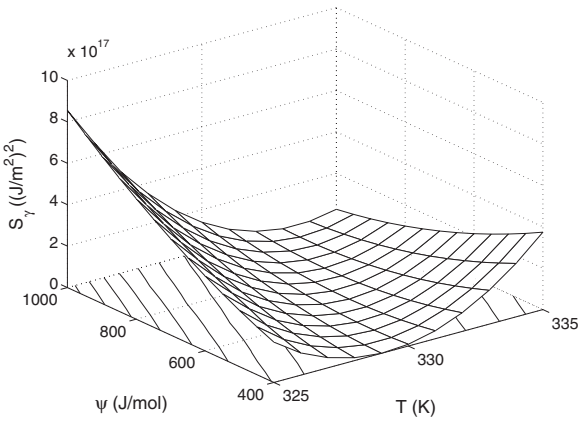

FIG. 7. The plot of $S_t(T,\psi)$ for t being the profile of the surface tension γ for the case of perturbing $T^\ell=1.02T_{\mathrm{eq}}$. The lines in the T-ψ plane are lines of constant value of $S_t(T,\psi)$

$$S_{\Gamma_{12}}(T,\psi)=\sum_{x^s}\left[\frac{\hat{c}'_{1,\mathrm{eq}}(x^s;T,\psi)}{\hat{c}'_1(x^s)}-\frac{\hat{c}'_{2,\mathrm{eq}}(x^s;T,\psi)}{\hat{c}'_2(x^s)}\right]^2, \tag{6.1}$$

where the prime indicates the derivative with respect to x^s.

$S_i(T,\psi)$ (where i is either γ or Γ_{12}) should reach the minimum at $T^s_{\{x^s\}}$ and $\psi^s_{\{x^s\}}$. We note however that neither $S_i(T,\psi)$ have a minimum at a single point (T^s,ψ^s). There is a whole generatrix curve of minima $C_i(T,\psi)=0$ so the plot of $S_i(T,\psi)$ is a valley. One can see it on Fig. 7. Every point of the generatrix curve is the minimum point of $S_i(T,\psi)$ along the direction "perpendicular" to this generatrix. If $\hat{p}_\parallel(x^s)$ or $\hat{c}'_1(x^s)$ and $\hat{c}'_2(x^s)$ represent the corresponding profiles for some equilibrium state $(T_{\mathrm{eq}},\psi_{\mathrm{eq}})$, then $S_i(T,\psi)=0$ and the generatrix is constant. Since these profiles are nonequilibrium profiles, the generatrix is not exactly constant but very close to it. Thus $C_i(T,\psi)=\partial S_i(T,\psi)/\partial w$, where w is a direction in the T-ψ plane which is perpendicular to generatrix. In fact, one should be careful speaking about directions, since no metric is defined in the T-ψ plane. Thus we cannot introduce $\boldsymbol{\nabla}_{T\psi}$ so that $C_i(T,\psi)=|\boldsymbol{\nabla}_{T\psi}S_i(T,\psi)|$. In fact, w can be any direction which does not coincide or does not almost coincide with the direction of generatrix. In practice we find that we can use $w=T$, while using $w=\psi$ gives less accurate results. Thus we determine the minimum curve from the equation

$$\frac{\partial S_i(T,\psi)}{\partial T}=0. \tag{6.2}$$

Thus one needs two quantities S_γ and S_Γ in order to determine $T^s_{\{x^s\}}$ and $\psi^s_{\{x^s\}}$ uniquely. The surface temperature and chemical potential difference $T^s_{\{x^s\}}$ and $\psi^s_{\{x^s\}}$ are determined from the intersection of two minimum curves of S_γ and S_Γ,

$$\left.\frac{\partial S_\gamma(T,\psi)}{\partial T}\right|_{T^s_{\{x^s\}},\psi^s_{\{x^s\}}}=0,$$

$$\left.\frac{\partial S_{\Gamma_{12}}(T,\psi)}{\partial T}\right|_{T^s_{\{x^s\}},\psi^s_{\{x^s\}}}=0. \tag{6.3}$$

TABLE IV. Surface temperatures (K) and chemical potential differences (J/mol) for the case of perturbing p^g.

	$p^g=1.02p_{\mathrm{eq}}$		$p^g=0.98p_{\mathrm{eq}}$	
Surface	T^s	ψ^s	T^s	ψ^s
$\{x^s\}$	330.796	683.87	329.059	696.52
x^c	330.8	684.68	329.063	697.22
x^γ	330.799	684.44	329.063	697.12
x^{c1}	330.804	685.19	329.065	697.46
x^{c2}	330.795	683.93	329.061	696.87

TABLE V. Surface temperatures (K) and chemical potential differences (J/mol) for the case of perturbing ζ^ℓ.

	$\zeta^\ell=1.02\zeta^\ell_{\mathrm{eq}}$		$\zeta^\ell=0.98\zeta^\ell_{\mathrm{eq}}$	
Surface	T^s	ψ^s	T^s	ψ^s
$\{x^s\}$	329.577	559.32	330.24	812.86
x^c	329.598	562.44	330.242	813.16
x^γ	329.584	560.5	330.253	814.67
x^{c1}	329.63	566.83	330.219	809.99
x^{c2}	329.554	556.3	330.278	817.99

We calculate the temperatures and the chemical potential differences for different nonequilibrium conditions. They are outlined in Tables III–V. The first row of each table, corresponding to $\{x^s\}$, gives T^s and ψ^s calculated from Eq. (6.3). The following rows, corresponding to different particular dividing surfaces, give T^s and ψ^s calculated from Eq. (5.8).

Note that T^s and ψ^s may be different from the continuous values in the interfacial region.

B. The nonequilibrium Gibbs surface

In this section we would like to verify that the surface quantities defined by Eq. (5.10) satisfy Eq. (6.4) with T^s and $\psi^s=\mu_1^s-\mu_2^s$ determined by Eq. (5.8) and Eq. (6.3),

$$\phi^s=\phi^s_{\mathrm{gibbs}}(T^s,\psi^s), \tag{6.4}$$

namely, with the definition Eq. (5.9),

$$\begin{aligned} h^s &= \mu_1^s c_1^s+\mu_2^s c_2^s+T^s s^s,\\ u^s &= \mu_1^s c_1^s+\mu_2^s c_2^s+\gamma^s+T^s s^s,\\ f^s &= \mu_1^s c_1^s+\mu_2^s c_2^s+\gamma^s,\\ g^s &= \mu_1^s c_1^s+\mu_2^s c_2^s, \end{aligned} \tag{6.5}$$

where the right-hand side is $\phi^s_{\mathrm{gibbs}}(T^s,\psi^s)$ of the corresponding quantity. Equation (6.5) is the nonequilibrium analog of equilibrium Equetion (5.1).

In order to analyze the measure of validity of Eq. (6.4) we construct the quantities

$$\begin{aligned} \mathcal{E}_{\phi_{\mathrm{gibbs}}}(T,\psi) &= \sum_{i\in\mathrm{surface}}\left[\frac{\phi^s(x_i^s)-\phi^s_{\mathrm{gibbs}}(x_i^s;T,\psi)}{\phi^s(x_i^s)}\right]^2,\\ \epsilon_{\phi_{\mathrm{gibbs}}}(x^s;T,\psi) &= \left|\frac{\phi^s(x^s)-\phi^s_{\mathrm{gibbs}}(x^s;T,\psi)}{\phi^s(x^s)}\right|, \end{aligned} \tag{6.6}$$

for each thermodynamic potential h, u, f, g. $\mathcal{E}_{\phi_{\mathrm{gibbs}}}$ gives the relative error of the determination of the surface quantity ϕ^s using the Gibbs excesses relations, Eq. (6.5), for all dividing surfaces together, while $\epsilon_{\phi_{\mathrm{gibbs}}}$ gives this error for a particular dividing surface. We build $\mathcal{E}_{\phi_{\mathrm{gibbs}}}(T,\psi)$ for $T=T^s_{\{x^s\}}$, $\psi=\psi^s_{\{x^s\}}$ determined from Eq. (6.3) only for the whole surface. We build $\epsilon_{\phi_{\mathrm{gibbs}}}(T,\psi)$ both for $T=T^s_{\{x^s\}}$, $\psi=\psi^s_{\{x^s\}}$ determined for the whole surface and for $T=T^s(x^s)$, $\psi=\psi^s(x^s)$ determined from Eq. (5.8) for particular dividing surface. The values of the corresponding errors are listed in Tables VI–VIII in the Appendix, and are found to be small.

As one can see, there is a variation in the value of the error for the different dividing surfaces. This has two reasons. The first reason for this is a slight variation in T^s and ψ^s from Tables III–V for different dividing surfaces. The variation of each excess potential corresponds to the variation of T^s and ψ^s through these surfaces. Thus so do the relative errors.

Another factor which influences the value of these errors is the actual value of an excess at a given dividing surface. If it is close to zero, then in the expression for ϵ the small value is in denominator and it gives the huge value for the error. Particularly, $g^s(x^c)\approx 0$ both in equilibrium and in nonequilibrium which makes the row corresponding to g at x^c be uninformative and one should not take into account these data.

We emphasize however that the overall error $\mathcal{E}_{\phi_{\mathrm{gibbs}}}$ represents the whole surface and thus does not suffer from the fact that some quantity is negligible at some dividing surface. There are such points for each potential ϕ, however their contribution to the whole error is negligible itself. So we can see that if the particular dividing surface is far from the zero point of ϕ, $\epsilon_{\phi_{\mathrm{gibbs}}}$ gives the good measure of the error. While if the particular dividing surface is close to the zero point of ϕ, $\epsilon_{\phi_{\mathrm{gibbs}}}$ fails to measure the error. One can see from Fig. 8 that the relative error $\epsilon_{\phi_{\mathrm{gibbs}}}$ indeed rises enormously at x^ϕ. Particularly because of this fact the definition of the excess quantities in [11] was different from Eq. (5.10).

We conclude that $\mathcal{E}_{\phi_{\mathrm{gibbs}}}$ is the most appropriate measure of the deviation of local equilibrium for the surface. From Tables VI–VIIIin the Appendix it then follows that even for such extreme conditions where the temperature difference across the box is up to 10^8 K/m the deviation is not more then a few thousandth. For less extreme conditions the deviation is correspondingly smaller. This is in agreement with the nonequilibrium surface being in local equilibrium.

Another possible test is to compare the absolute error $|\phi^s(x^s)-\phi^s_{\mathrm{gibbs}}(x^s;T,\psi^s)|$ with the deviation $\sigma_{\phi_{\mathrm{gibbs}}}(T,\psi)$ defined in Eq. (5.12). The calculations show that for the particular dividing surfaces the former quantity does not exceed the latter, which indicates that all the absolute errors are actually within the trust region.

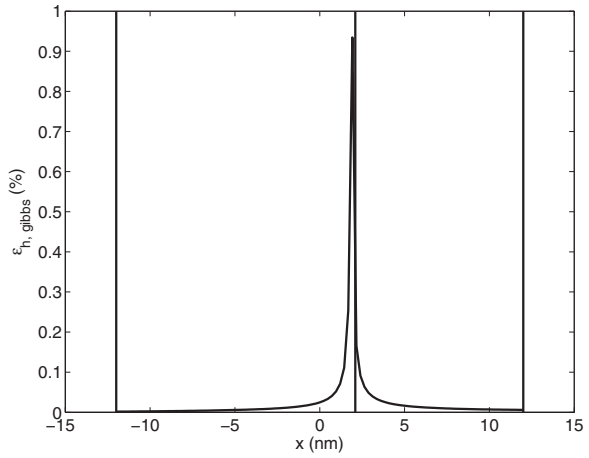

FIG. 8. The relative error $\epsilon_{h_{\mathrm{gibbs}}}(x^s;T^s_{\{x^s\}},\psi^s_{\{x^s\}})$ for the case of perturbing $T^\ell=1.02T_{\mathrm{eq}}$. The vertical lines indicate the surface boundaries and x^h dividing surfaces.

C. Equilibrium tables

In this section we verify the possibility to determine all properties of a nonequilibrium surface from equilibrium tables at the surface's T^s and ψ^s. The surface chemical potentials μ_1^s and μ_2^s are already defined as their equilibrium values by Eq. (5.9). So in this section we will verify the relation

$$\phi^s=\phi^s_{\mathrm{eq}}(T^s,\psi^s) \tag{6.7}$$

As in Sec. VI B we compare the actual excess of a thermodynamic potential with the corresponding equilibrium value at given temperature and chemical potential of the surface. Before we do this a note has to be made.

Under nonequilibrium conditions the profile of a quantity ϕ^s is shifted with respect to the equilibrium one. One can see this in the example for $\phi=h$ in Fig. 9. The reason for this are the fluxes caused by the nonequilibrium perturbation. The whole surface is therefore shifted. One can clearly see that comparing the positions of the particular dividing surfaces on Fig. 4 and Fig. 5. So the direct comparison of the profiles should be done not in the observer's frame of reference (OFO, which is used in all other calculations), but in the *surface's frame of reference* (SFO). The SFO is simply shifted with respect to the OFO, depending on the rate of nonequilibrium perturbations. Zero of the SFO is chosen at the reference surface, which can be either the equimolar surface, or any other physically sensible surface. If $x^\ominus$ is the position of this surface in OFO and $\phi^s_{\mathrm{OFO}}(x^s_{\mathrm{OFO}})$ is the profile of ϕ^s in OFO, then $\phi^s_{\mathrm{SFO}}(x^s_{\mathrm{SFO}})\equiv\phi^s_{\mathrm{OFO}}(x^s_{\mathrm{OFO}})=\phi^s_{\mathrm{OFO}}(x^s_{\mathrm{SFO}}+x^\ominus)$ is the profile of ϕ^s in SFO.

We can now determine the equilibrium state to which the nonequilibrium one should correspond. Consider the following definitions of $\mathcal{E}_{\phi_{\mathrm{table}}}$ and $\epsilon_{\phi_{\mathrm{table}}}$ which have the same meaning as in Eq. (6.6):

$$\mathcal{E}_{\phi_{\mathrm{table}}}(T,\psi)=\sum_{i\in\mathrm{surface}}\left[\frac{\phi^s(x^s_i)-\phi^s_{\mathrm{eq}}(x^s_i+x^\ominus_{\mathrm{eq}}-x^\ominus;T,\psi)}{\phi^s(x^s_i)}\right]^2,$$

$$\epsilon_{\phi_{\mathrm{table}}}(x^s;T,\psi)=\left|\frac{\phi^s(x^s)-\phi^s_{\mathrm{eq}}(x^s;T,\psi)}{\phi^s(x^s)}\right|, \tag{6.8}$$

for each thermodynamic potential h, u, f, g. $x^\ominus$ and $x^\ominus_{\mathrm{eq}}$ are the nonequilibrium and equilibrium positions of the reference surface in OFO. The set $\{x^s_i\}$ is the nonequilibrium surface grid and is used for both profiles. Since the width of an equilibrium surface may not be the same as the nonequilibrium one, the summation may exceed the formal boundaries of the equilibrium surface. This is not a problem, however, since the equilibrium profile ψ^s_{eq} is the line with constant slope everywhere, as well as beyond the formal boundaries. We do not shift the surface grid in the definition of $\epsilon_{\phi_{\mathrm{table}}}(x^s;T,\psi)$ because in that notation x^s means the particular dividing surface, while x^s_i means the point of the surface grid.

The values of the corresponding errors are listed in Tables IX–XI in the Appendix, and, though somewhat larger then those in Sec. VI B, are still small. As in Sec. VI B we see that for the equimolar surface the relative error in g is huge.

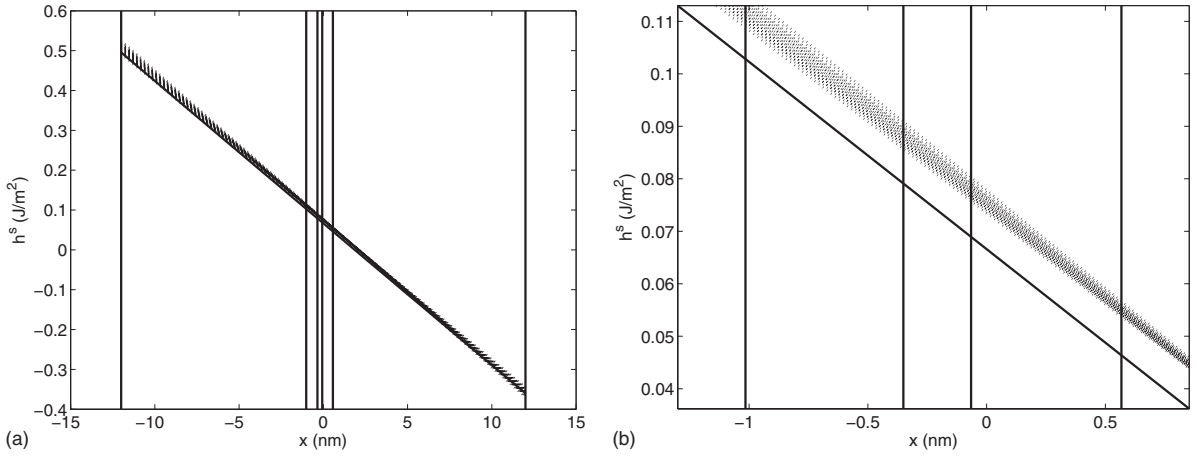

FIG. 9. Nonequilibrium profile of h^s for the case of perturbing $T^\ell=1.02T_{\mathrm{eq}}$ (solid line) compared to the profiles of h^s_{eq} calculated from the equilibrium tables for different T_{eq} and ψ_{eq} (dotted lines). The vertical lines indicate the surface boundaries and dividing surfaces for the nonequilibrium case.

TABLE VI. Gibbs excesses relative error for the case of perturbing T^ℓ in percent.

		$T^\ell = 1.02T_{\mathrm{eq}}$		$T^\ell = 0.98T_{\mathrm{eq}}$	
ϕ	Error	For $T^s_{\{x^s\}}$, $\psi^s_{\{x^s\}}$	For $T^s(x^s)$, $\psi^s(x^s)$	For $T^s_{\{x^s\}}$, $\psi^s_{\{x^s\}}$	For $T^s(x^s)$, $\psi^s(x^s)$
h	$\mathcal{E}$	0.01328	—	0.033276	—
	$\epsilon_\phi(x^c)$	0.023799	0.023419	0.064597	0.065002
	$\epsilon_\phi(x^\gamma)$	0.020605	0.020737	0.056585	0.057148
	$\epsilon_\phi(x^{c1})$	0.035878	0.033571	0.085212	0.085204
	$\epsilon_\phi(x^{c2})$	0.015606	0.016541	0.047847	0.048578
u	$\mathcal{E}$	0.0071257	—	0.026714	—
	$\epsilon_\phi(x^c)$	0.016729	0.016462	0.045109	0.045392
	$\epsilon_\phi(x^\gamma)$	0.015059	0.015156	0.041048	0.041457
	$\epsilon_\phi(x^{c1})$	0.022033	0.020616	0.054286	0.05428
	$\epsilon_\phi(x^{c2})$	0.012161	0.012889	0.036244	0.036797
f	$\mathcal{E}$	0.20039	—	0.12983	—
	$\epsilon_\phi(x^c)$	7.3727	7.3666	8.7959	8.799
	$\epsilon_\phi(x^\gamma)$	1.9809	1.981	2.2605	2.2602
	$\epsilon_\phi(x^{c1})$	1.6966	1.6881	2.5586	2.5602
	$\epsilon_\phi(x^{c2})$	0.65429	0.65354	1.0109	1.0095
g	$\mathcal{E}$	0.36323	—	0.15487	—
	$\epsilon_\phi(x^c)$	272.37	272.15	73.468	73.494
	$\epsilon_\phi(x^\gamma)$	2.7241	2.7242	3.2313	3.2309
	$\epsilon_\phi(x^{c1})$	1.4054	1.3983	1.9592	1.9605
	$\epsilon_\phi(x^{c2})$	0.72857	0.72773	1.1818	1.1802

There is the same reason for this, namely that $g^s(x_c) \approx 0$ both in equilibrium and in nonequilibrium. This again makes the row corresponding to g at x^c be uninformative and one should not take into account these data.

As discussed in Sec. VI B $\mathcal{E}_{\phi_{\mathrm{table}}}(T,\psi)$ is now the appropriate measure of the validity of local equilibrium. In view of the small size of this quantity we similarly conclude that Eq. (6.7) is satisfied in good approximation. This again supports that the nonequilibrium surface as described by Gibbs excess densities is in local equilibrium.

VII. CONCLUSIONS

The article continued the verification of the validity of local equilibrium for the Gibbs surface started in [11]. We consider a binary mixture of cyclohexane and *n*-hexane and describe in detail how to implement the general analysis presented in the first article [1] to stationary states. We give a numerical procedure to solve the resulting system of differential equations. The profiles of continuous variables obtained are presented in Sec. IV and in the first article. We see, in particular, that a two-component mixture develops a temperature profile in the surface region which is similar to the temperature profile obtained for a one-component system [21]. Another characteristic of a binary mixture is the difference $\psi = \mu_1 - \mu_2$ between the chemical potentials of the components. The behavior of the profile of ψ in nonequilibrium steady states shows that it has different values in the two bulk phases and we observe a transition from one value to the other in the surface region.

We then proceed to verify the local equilibrium property of the Gibbs surface. This property means that a surface under nonequilibrium steady-state conditions can be described as an equilibrium one in terms of Gibbs excess densities. We have discussed the meaning of the surface quantities in nonequilibrium and established the systematic procedure to obtain them. We were in particular focused on (i) the existence of the surface temperature and chemical potentials which are independent of the choice of the dividing surface; (ii) the validity of the relations between thermodynamic Gibbs excesses for a nonequilibrium surface; (iii) the correspondence between the nonequilibrium and equilibrium properties of the surface. It was possible to verify that these properties are valid for all choices of the dividing surface with a good accuracy. Similar results were obtained for the one-component system in Ref. [11].

The solution procedure is numerical, and contains therefore a certain error. We may not expect this error to be negligible, not only because of numerical inaccuracy, but in particular also because of the nonequilibrium nature of the system. All these errors contribute to the overall measure of the deviation $\mathcal{E}_\phi$. As this quantity is not more then a few thousandth for very extreme boundary conditions, we consider this a satisfactory verification of local equilibrium.

The main part of the analysis in the interfacial region is the introduction of the excesses of thermodynamic densities, which are constructed with the help of extrapolated bulk profiles. In contrast to equilibrium, nonequilibrium bulk profiles are not constants, and therefore their extrapolation to the surface region is not always accurate. The accuracy of ex-

trapolation lowers when the surface width increases. Apparent small deviations from local equilibrium are therefore to some extent an artifact of the inaccuracy of the extrapolation.

In the description of the surface excess densities it may happen that for a particular choice of the dividing surface not one but several of the excesses are negligible. This increases the relative error enormously while the absolute error remains finite and more or less constant. In order to avoid this problem we consider the excesses for all dividing surfaces together, rather then for a particular dividing surface. Particularly, in [11] the definition of the excess Gibbs energy was chosen differently because this excess was very small for the equimolar surface. We have shown in this paper why this is not needed.

One can see from these data that within different ways of perturbing mixture from equilibrium the biggest error comes when one perturbs the temperature on the liquid side. This is the most extreme condition for the mixture being in nonequilibrium. While the relative temperature perturbation is only 2%, the resulting temperature gradient is about 10^8 K/m which is very far beyond ordinary nonequilibrium conditions. The other perturbations make the validity of local equilibrium for the surface more precise. Similarly smaller perturbations make the validity of local equilibrium also more precise.

We therefore conclude that the local equilibrium of the surface is valid with a reasonable accuracy also under extreme temperature gradients for binary mixtures. For the description of transport through and into surfaces this verifies that the use of nonequilibrium thermodynamics as done in, for instance, Refs. [7–10], is appropriate. For the application to industrial processes this is an important simplification, which is of great importance.

ACKNOWLEDGMENTS

The authors want to thank Eivind Johannessen for clarifications of his work and for advice. We are also grateful to NFR for Storforks Grant No. 167336/V30.

APPENDIX A: EXCESSES ERRORS

1. Gibbs excesses relative errors

Tables VI–VIII list the Gibbs excesses relative errors for perturbing T^ℓ, p^g, and ζ^ℓ.

2. Equilibrium table excesses relative errors

Tables IX–XI list the equilibrium table excesses relative errors for perturbing T^ℓ, p^9, and ζ^ℓ.

TABLE VII. Gibbs excesses relative error for the case of perturbing p^g in percent.

		$p^g=1.02p_{\mathrm{eq}}$		$p^g=0.98p_{\mathrm{eq}}$	
ϕ	Error	For $T^s_{\{x^s\}}$, $\psi^s_{\{x^s\}}$	For $T^s(x^s)$, $\psi^s(x^s)$	For $T^s_{\{x^s\}}$, $\psi^s_{\{x^s\}}$	For $T^s(x^s)$, $\psi^s(x^s)$
h	$\mathcal{E}$	0.0013703	—	0.0019532	—
	$\epsilon_\phi(x^c)$	0.0018964	0.0022352	0.0011722	0.00088793
	$\epsilon_\phi(x^\gamma)$	0.0017063	0.0019978	0.0010683	0.00083823
	$\epsilon_\phi(x^{c1})$	0.0025175	0.0030049	0.0015513	0.0010756
	$\epsilon_\phi(x^{c2})$	0.0014259	0.0016451	0.00090372	0.00076269
u	$\mathcal{E}$	0.00041867	—	0.00033213	—
	$\epsilon_\phi(x^c)$	0.0013316	0.0015695	0.00081921	0.00062057
	$\epsilon_\phi(x^\gamma)$	0.00124	0.001452	0.00077388	0.00060722
	$\epsilon_\phi(x^{c1})$	0.0015926	0.001901	0.00096161	0.00066669
	$\epsilon_\phi(x^{c2})$	0.001093	0.001261	0.00069529	0.00058679
f	$\mathcal{E}$	0.043422	—	0.033692	—
	$\epsilon_\phi(x^c)$	1.4194	1.4152	1.2845	1.2884
	$\epsilon_\phi(x^\gamma)$	0.3884	0.38805	0.37919	0.3795
	$\epsilon_\phi(x^{c1})$	0.40171	0.39739	0.30303	0.30621
	$\epsilon_\phi(x^{c2})$	0.13128	0.1311	0.13976	0.13952
g	$\mathcal{E}$	0.08442	—	0.021892	—
	$\epsilon_\phi(x^c)$	28.236	28.152	48.786	48.935
	$\epsilon_\phi(x^\gamma)$	0.56258	0.56208	0.54645	0.5469
	$\epsilon_\phi(x^{c1})$	0.3187	0.31528	0.24447	0.24704
	$\epsilon_\phi(x^{c2})$	0.15021	0.15001	0.1583	0.15802

TABLE VIII. Gibbs excesses relative error for the case of perturbing ζ^ℓ in percent.

		$\zeta^\ell = 1.02\zeta^\ell_{\mathrm{eq}}$		$\zeta^\ell = 0.98\zeta^\ell_{\mathrm{eq}}$	
ϕ	Error	For $T^s_{\{x^s\}}$, $\psi^s_{\{x^s\}}$	For $T^s(x^s)$, $\psi^s(x^s)$	For $T^s_{\{x^s\}}$, $\psi^s_{\{x^s\}}$	For $T^s(x^s)$, $\psi^s(x^s)$
h	$\mathcal{E}$	0.00035435	—	0.0011482	—
	$\epsilon_\phi(x^c)$	0.0023134	0.0028072	0.0042669	0.0042419
	$\epsilon_\phi(x^\gamma)$	0.0021873	0.0026065	0.0039043	0.0039484
	$\epsilon_\phi(x^{c1})$	0.0028054	0.0035457	0.0054811	0.0052479
	$\epsilon_\phi(x^{c2})$	0.0020102	0.0023063	0.0033597	0.0035215
u	$\mathcal{E}$	0.00040969	—	0.0015073	—
	$\epsilon_\phi(x^c)$	0.0016206	0.0019665	0.0029893	0.0029717
	$\epsilon_\phi(x^\gamma)$	0.0015861	0.0018901	0.0028345	0.0028665
	$\epsilon_\phi(x^{c1})$	0.0017517	0.0022139	0.0034446	0.003298
	$\epsilon_\phi(x^{c2})$	0.0015408	0.0017677	0.0025842	0.0027086
f	$\mathcal{E}$	0.0063873	—	0.0026805	—
	$\epsilon_\phi(x^c)$	0.17101	0.15419	0.033343	0.034999
	$\epsilon_\phi(x^\gamma)$	0.014471	0.015093	0.023261	0.022844
	$\epsilon_\phi(x^{c1})$	0.15718	0.13049	0.066572	0.055875
	$\epsilon_\phi(x^{c2})$	0.062407	0.065842	0.037405	0.042978
g	$\mathcal{E}$	0.013595	—	0.0004864	—
	$\epsilon_\phi(x^c)$	5.3413	4.816	0.77321	0.8116
	$\epsilon_\phi(x^\gamma)$	0.021	0.021903	0.033471	0.032872
	$\epsilon_\phi(x^{c1})$	0.12645	0.10498	0.052965	0.044454
	$\epsilon_\phi(x^{c2})$	0.071253	0.075175	0.042467	0.048795

TABLE IX. Equilibrium table excesses relative error for the case of perturbing T^ℓ in percent.

		$T^\ell = 1.02T_{\mathrm{eq}}$		$T^\ell = 0.98T_{\mathrm{eq}}$	
ϕ	Error	For $T^s_{\{x^s\}}$, $\psi^s_{\{x^s\}}$	For $T^s(x^s)$, $\psi^s(x^s)$	For $T^s_{\{x^s\}}$, $\psi^s_{\{x^s\}}$	For $T^s(x^s)$, $\psi^s(x^s)$
h	$\mathcal{E}$	0.67514	—	0.21243	—
	$\epsilon_\phi(x^c)$	1.1052	1.1012	0.51202	0.50951
	$\epsilon_\phi(x^\gamma)$	0.0062189	0.0050111	0.074177	0.071345
	$\epsilon_\phi(x^{c1})$	8.5087	8.4753	6.4524	6.4581
	$\epsilon_\phi(x^{c2})$	3.9073	3.8963	6.1946	6.1882
u	$\mathcal{E}$	0.32181	—	0.23381	—
	$\epsilon_\phi(x^c)$	0.77685	0.77406	0.35744	0.3558
	$\epsilon_\phi(x^\gamma)$	0.0043659	0.00366	0.053575	0.051756
	$\epsilon_\phi(x^{c1})$	5.2257	5.2046	4.1104	4.1143
	$\epsilon_\phi(x^{c2})$	3.0451	3.0361	4.692	4.6875
f	$\mathcal{E}$	0.0046133	—	0.0035049	—
	$\epsilon_\phi(x^c)$	6.6737	6.67	8.0558	8.0599
	$\epsilon_\phi(x^\gamma)$	7.242	7.2428	0.37022	0.37236
	$\epsilon_\phi(x^{c1})$	15.74	15.7	25.631	25.642
	$\epsilon_\phi(x^{c2})$	13.328	13.306	20.092	20.077
g	$\mathcal{E}$	0.0017615	—	0.001069	—
	$\epsilon_\phi(x^c)$	246.55	246.41	67.29	67.32
	$\epsilon_\phi(x^\gamma)$	9.9591	9.9604	0.52885	0.53228
	$\epsilon_\phi(x^{c1})$	13.038	13.006	19.627	19.635
	$\epsilon_\phi(x^{c2})$	14.84	14.817	23.49	23.472

TABLE X. Equilibrium table excesses relative error for the case of perturbing p^g in percent.

		$p^g=1.02p_{\mathrm{eq}}$		$p^g=0.98p_{\mathrm{eq}}$	
ϕ	Error	For $T^s_{\{x^s\}}$, $\psi^s_{\{x^s\}}$	For $T^s(x^s)$, $\psi^s(x^s)$	For $T^s_{\{x^s\}}$, $\psi^s_{\{x^s\}}$	For $T^s(x^s)$, $\psi^s(x^s)$
h	$\mathcal{E}$	0.26501	—	1.3628	—
	$\epsilon_\phi(x^c)$	0.79783	0.80083	0.90685	0.90956
	$\epsilon_\phi(x^\gamma)$	1.4549	1.457	1.2481	1.2505
	$\epsilon_\phi(x^{c1})$	1.3056	1.2901	2.0582	2.0702
	$\epsilon_\phi(x^{c2})$	2.3955	2.3962	0.069749	0.072757
u	$\mathcal{E}$	0.047434	—	0.20486	—
	$\epsilon_\phi(x^c)$	0.5599	0.56232	0.63362	0.63569
	$\epsilon_\phi(x^\gamma)$	1.0571	1.0589	0.90402	0.90589
	$\epsilon_\phi(x^{c1})$	0.82642	0.81614	1.2756	1.2832
	$\epsilon_\phi(x^{c2})$	1.836	1.8368	0.053565	0.055977
f	$\mathcal{E}$	0.003912	—	0.0035128	—
	$\epsilon_\phi(x^c)$	1.218	1.2144	1.1886	1.1919
	$\epsilon_\phi(x^\gamma)$	4.7735	4.775	2.1767	2.1788
	$\epsilon_\phi(x^{c1})$	7.4201	7.3951	2.2105	2.2271
	$\epsilon_\phi(x^{c2})$	5.5423	5.5439	1.9531	1.9467
g	$\mathcal{E}$	0.0013182	—	0.00041813	—
	$\epsilon_\phi(x^c)$	24.251	24.157	45.122	45.27
	$\epsilon_\phi(x^\gamma)$	6.9147	6.9164	3.1371	3.1398
	$\epsilon_\phi(x^{c1})$	5.8866	5.8671	1.7835	1.7967
	$\epsilon_\phi(x^{c2})$	6.3419	6.3437	2.212	2.2049

TABLE XI. Equilibrium table excesses relative error for the case of perturbing ζ^ℓ in percent.

		$\zeta^\ell=1.02\zeta^\ell_{\mathrm{eq}}$		$\zeta^\ell=0.98\zeta^\ell_{\mathrm{eq}}$	
ϕ	Error	For $T^s_{\{x^s\}}$, $\psi^s_{\{x^s\}}$	For $T^s(x^s)$, $\psi^s(x^s)$	For $T^s_{\{x^s\}}$, $\psi^s_{\{x^s\}}$	For $T^s(x^s)$, $\psi^s(x^s)$
h	$\mathcal{E}$	0.093953	—	0.20248	—
	$\epsilon_\phi(x^c)$	0.85205	0.86417	0.83511	0.8363
	$\epsilon_\phi(x^\gamma)$	1.5557	1.5598	1.1532	1.1601
	$\epsilon_\phi(x^{c1})$	0.24334	0.33902	0.26902	0.23261
	$\epsilon_\phi(x^{c2})$	1.265	1.2405	1.2654	1.3065
u	$\mathcal{E}$	0.068203	—	0.24097	—
	$\epsilon_\phi(x^c)$	0.59647	0.60537	0.585	0.58586
	$\epsilon_\phi(x^\gamma)$	1.1278	1.1311	0.8372	0.84222
	$\epsilon_\phi(x^{c1})$	0.15127	0.21168	0.169	0.14618
	$\epsilon_\phi(x^{c2})$	0.96943	0.95081	0.97333	1.0049
f	$\mathcal{E}$	0.0026249	—	0.0035651	—
	$\epsilon_\phi(x^c)$	0.095422	0.080499	0.18152	0.18276
	$\epsilon_\phi(x^\gamma)$	4.6443	4.6454	2.382	2.3867
	$\epsilon_\phi(x^{c1})$	2.3591	2.2252	2.7907	2.8466
	$\epsilon_\phi(x^{c2})$	1.6382	1.5842	1.897	1.9858
g	$\mathcal{E}$	0.00098739	—	0.0010871	—
	$\epsilon_\phi(x^c)$	3.025	2.5143	4.2062	4.237
	$\epsilon_\phi(x^\gamma)$	6.7404	6.7414	3.4276	3.4343
	$\epsilon_\phi(x^{c1})$	1.8975	1.7901	2.2203	2.2648
	$\epsilon_\phi(x^{c2})$	1.8705	1.8088	2.1538	2.2546

[1] K. S. Glavatskiy and D. Bedeaux, Phys. Rev. E **77**, 061101 (2008).
[2] J. S. Rowlinson and B. Widom, *Molecular Theory of Capillarity* (Clarendon Press, Oxford, 1982).
[3] J. Williard Gibbs, *The Scientific Papers of J. Williard Gibbs* (Ox Bow Press, Woodbridge, CT, 1993).
[4] G. Bakker, *Kapillaritat und Oberflachenspannung*, Handbuch der Experimental-Physik Vol. 6 (Akad. Verlag, Leipzig, 1928).
[5] E. A. Guggenheim, *Thermodynamics*, 5th ed. (North-Holland, Amsterdam, 1967).
[6] R. Defay and I. Prigogine, *Surface Tension and Adsorption* (Longman, London, 1966).
[7] D. Bedeaux, A. M. Albano, and P. Mazur, Physica A **82**, 438 (1975).
[8] D. Bedeaux, Adv. Chem. Phys. **64**, 47 (1986).
[9] A. M. Albano and D. Bedeaux, Physica A **147**, 407 (1987).
[10] S. Kjelstrup and D. Bedeaux, *Non-Equilibrium Thermodynamics of Heterogeneous Systems*, Series on Advances in Statistical Mechanics Vol. 16 (World Scientific, Singapore, 2008).
[11] E. Johannessen and D. Bedeaux, Physica A **330**, 354 (2003).
[12] A. Røsjorde, D. W. Fossmo, D. Bedeaux, S. Kjelstrup, and B. Hafskjold, J. Colloid Interface Sci. **232**, 178 (2000).
[13] J.-M. Simon, S. Kjelstrup, D. Bedeaux, and B. Hafskjold, J. Phys. Chem. B **108**, 7186 (2004).
[14] J. Ge, S. Kjelstrup, D. Bedeaux, J. M. Simon, and B. Rousseau, Phys. Rev. E **75**, 061604 (2007).
[15] B. Hafskjold and S. Kjelstrup, Ind. Eng. Chem. Res. **35**, 4203 (1996).
[16] S. Kjelstrup and B. Hafskjold, Ind. Eng. Chem. Res. **35**, 4203 (1996).
[17] M.-L. Olivier, Ph.D. thesis, Norwegian University of Science and Technology, Department of Refrigeration and Air Conditioning, Trondheim, Norway, 2002.
[18] M.-L. Olivier, J.-D. Rollier, and S. Kjelstrup, Colloids Surf., A **210**, 199 (2002).
[19] J. M. Simon, D. Bedeaux, S. Kjelstrup, J. Xu, and E. Johannessen, J. Phys. Chem. B **110**, 18528 (2006).
[20] S. R. de Groot and P. Mazur, *Non-Equilibrium Thermodynamics* (Dover, New York, 1984).
[21] D. Bedeaux, E. Johannessen, and A. Rosjorde, Physica A **330**, 329 (2003).
[22] L. F. Shampine, M. W. Reichelt, and J. Kierzenka, 2003, http://www.mathworks. com/bvp_tutorial.
[23] *CRC Handbook of Chemistry and Physics*, 88th edition, edited by David R. Lide (Taylor and Francis, London 2008).
[24] Carl L. Yaws, *Yaws'Handbook of Thermodynamic and Physical Properties of Chemical Compounds* (Knovel, New York, 2003).
[25] Q. Dong, K. N. Marsh, B. E. Gammon, and A. K. R. Dewan, *Transport Properties and Related Thermodynamic Data of Binary Mixtures* (DIPPR, Provo, Utah, 1996), Vol. 3.